Andreev–Saint-James reflections: A probe of cuprate superconductors

Guy Deutscher*

School of Physics and Astronomy, Sackler Faculty of Exact Sciences, Tel Aviv University, Ramat Aviv, Tel Aviv 69978, Israel

(Published 23 March 2005)

Electrical transport through a normal-metal/superconductor contact at biases smaller than the energy gap can occur via the reflection of an electron as a hole of opposite wave vector. The same mechanism of electron-hole reflection gives rise to low-energy states at the surface of unconventional superconductors having nodes in their order parameter. The occurrence of electron-hole reflections at normal-metal/superconductor interfaces was predicted independently by Saint-James and de Gennes and by Andreev, and their spectroscopic features were discussed in detail by Saint-James in the early sixties. They are generally called Andreev reflections but, in view of the literature, will here be referred to as Andreev–Saint-James (ASJ) reflections. This review presents a historical review of ASJ reflections and spectroscopy in conventional superconductors, and reviews their application to the high-T_c cuprates. The occurrence of ASJ reflections in all studied cuprates is well documented for a broad range of doping levels, implying that there is no large asymmetry between electrons and holes near the Fermi level in the superconducting state. In the underdoped regime, where the pseudogap phenomenon has been observed by other methods such as nuclear magnetic resonance (NMR), angular-resolved photoemission spectroscopy (ARPES), and Giaever tunneling, gap values obtained from ASJ spectroscopy are smaller than pseudogap values, indicating a lack of coherence in the pseudogap energy range. Low-energy surface bound states have been observed in all studied hole-doped cuprates, in agreement with a dominant *d*-wave symmetry order parameter. Results are mixed for electron-doped cuprates. In overdoped $YBa_2Cu_3O_{7-\delta}$ ($\delta<0.08$) and $La_{2-x}Sr_xCuO_4$, ASJ spectroscopy is consistent with the presence of an additional imaginary component of the order parameter. Results of ASJ spectroscopy under applied magnetic fields are also reviewed. A short section at the end is devoted to some recent results on spin effects.

CONTENTS

I. Introduction 110
II. Solution of the Bogoliubov–de Gennes Equations near an N/S Interface 112
A. The case of a normal slab in contact with a semi-infinite superconductor 112
B. The case of a normal layer sandwiched between two superconductors: Effect of a phase difference 113
C. Surface bound states in a *d*-wave superconductor 114
III. Conductance Characteristics of Sharvin Contacts 114
A. Sharvin contacts as a tool for ASJ spectroscopy 114
B. Fabrication of Sharvin contacts 115
C. Blonder-Tinkham-Klapwijk model 115
1. Case of a clean interface 116
2. Contacts with a finite transparency 116
D. High-temperature superconductor point-contact results for an antinodal orientation 117
1. Early experiments on high-quality single-crystal YBCO samples 117
2. Effect of *d*-wave symmetry for an antinodal direction 117
E. Renormalization of the Fermi velocity 118
1. The problem of the small Fermi velocity mismatch 118
2. Solution to the problem 119
F. Summary 120
IV. ASJ Surface Bound States 120
A. Zero-bias conductance peaks and *d*-wave symmetry 120
1. Results of Kashiwaya *et al.* for the (110) orientation 120
2. Results of Kashiwaya *et al.* for arbitrary orientations 121
B. Experimental results 121
1. Low-Z (110) contacts 121
2. High-Z (110) contacts 122
3. High-Z (110) contacts under magnetic fields 124
V. ASJ Spectroscopy and the Pseudogap Issue 125
A. Manifestations and possible origins of the pseudogap 125
B. ASJ spectroscopy in the pseudogap regime 126
C. Compatibility of ASJ reflections and pseudogap models 127
1. Resonating valence bond and other models emphasizing strong correlation effects 127
2. The semiconductor-superconductor and strong-coupling models 128
3. Two-gap model 129
4. Some comments on the pseudogap 129
VI. Symmetry Studies and Spin Effects 130
A. ASJ bound states under applied fields 130
B. Doping effect on the symmetry 131
C. Proximity effect on the symmetry 132
D. Spin effects 132
VII. Conclusions 133
Acknowledgments 133
References 133

*Electronic address: guyde@tau.ac.il

I. INTRODUCTION

When an electron moving in a normal metal (N) with momentum k hits an interface with a superconductor (S), it is reflected as a hole of equal momentum if its kinetic energy measured from the Fermi level is smaller than the energy gap Δ of S. Because of its negative effective mass, the reflected hole has a velocity opposite to that of the incoming electron and carries charge current in the same direction. This process, known today as an Andreev reflection (Andreev, 1964), is a key feature of the solution of the Bogoliubov–de Gennes equations (de Gennes, 1966), based on the Bogoliubov transformation (Bogoliubov, 1947, 1958), near an N/S interface. A solution of these equations was first given by de Gennes and Saint-James (1963), who applied it to the case of an N/S bilayer. The special reflections decrease thermal transport across an N/S interface, as shown by Andreev (1964) and control the density of states in an N/S bilayer, as discussed in detail by Saint-James (1964).

Andreev was interested in heat transport in the intermediate state of a type-I superconductor and showed that domain walls provide a resistance to this flow because of the electron-hole reflection mechanism. This is why the thermal resistance in the intermediate state is higher than in the Meissner state, as observed by Mendelssohn and Olsen (1950). Andreev was able to fit quantitatively the detailed heat-transport measurements of Zavaritskii (1960). de Gennes and Saint-James, on the other hand, were interested in the density of states in a system consisting of a normal slab of thickness d_N in close electrical contact with a semi-infinite superconductor. They showed that the density of states has a series of peaks below Δ because of the existence of finite-energy bound states in N. For large enough values of d_N, these peaks are located at energies that are multiples of $(\hbar v_F/4d_N)$, where v_F is the Fermi velocity in N. Saint-James (1964) remarks that the interlevel distance is half of that for an electron in a potential well and explains that this is because a complete cycle comprises two electron-hole reflections at the N/S interface and two specular reflections at the outer surface of N. In this cycle, the quasiparticle has both an electronlike and a holelike character.

The Andreev 1964 paper was, and still is, widely cited, perhaps because it explained a specific and observed physical phenomenon. The slightly earlier paper of de Gennes and Saint-James (1963) is less often cited, and the simultaneous paper of Saint-James (1964) is known only to some experts in the field. It is an excellent paper, which I highly recommend reading. Its emphasis on the spectroscopic aspects of the electron-hole reflections is very close to the topic of the present paper, the use of these reflections for the spectroscopic study of high-temperature superconductors. After consulting with some colleagues, I decided for this reason to use in this review the terms Andreev–Saint-James (ASJ) reflections and spectroscopy.

Another curious aspect of the history of ASJ reflections is that it took almost 20 years before it was shown theoretically that they enhance the electrical conductance of N/S contacts at biases below the gap, in contrast with the *reduction* of the thermal conductance. This enhancement of the electrical conductance appears obvious to us today. An electron coming in from the N side at energies smaller than Δ cannot propagate inside S; only Cooper pairs may do so. The reflected hole ensures current conservation. A charge of $2e$ then flows across the interface, which corresponds to an increase in the conductance of the contact by a factor of 2 compared to that in the normal state, or at biases much larger than the gap. The detailed way in which the process occurs involves the creation of electron and hole excitations in S near the interface, which recombine into pairs over the coherence length of the superconductor. Pankove (1966) reported an enhanced electrical conductance of N/S contacts below the gap. His observations on pressure contacts between Al and Nb are clear: "When a contact is made between a normal metal and a superconductor, the *V-I* characteristic of the contact shows an initial region of high conductance with an abrupt change to a region of lower conductance" (Pankove, 1966, p. 406). However, Pankove did not relate his observation to the works of Andreev and de Gennes and Saint-James. Likewise, his observations were not noted by theorists. Griffin and Demers (1971) were the first to calculate the quasiparticle transmission probability for excitations going from a normal to a superconducting region for N/S contacts of various transparencies, but did not take into consideration the electron-hole reflection mechanism and the corresponding flow of pairs. It was not until 1980 that Zaitsev (1980) calculated an enhanced conductance below the gap, and only in 1982 did Blonder, Tinkham, and Klapwijk (Blonder *et al.*, 1982) give a complete theoretical discussion, including the effect of an imperfect (not fully transparent) interface, and successfully compare their predictions to measurements performed on point contacts.

Sharvin (1965) was the first to note that the electrical resistance of an ideal intermetallic contact of a size smaller than the electronic mean free path is determined by the number of quantum channels through the contact. These contacts, called *Sharvin contacts* or *point contacts*, are the ideal tool for the study of ASJ reflections, for reasons that will be reviewed later in great detail. However, Sharvin apparently did not use them for that purpose, another strange twist in the history of ASJ reflections. Pankove contacts were actually Sharvin contacts, and he calculates that their size is of about 50 Å, a typical point contact size.

The transition between the regions of higher and lower conductance noted by Pankove occurs when the bias across the contact is equal to the energy gap. ASJ reflections are therefore a useful tool for the determination of the gap. Blonder *et al.* (1982) made this tool a quantitative one by taking into account the nonideal nature of the contact, including the effect of a thin insulating barrier and that of a mismatch of the Fermi velocities between the two metals. Yet their work had only a limited impact on the study of low-temperature super-

conductors, perhaps because it came much later than the full development of tunneling theory (McMillan and Rowell, 1969) and also, I suppose, because the controlled fabrication of thin tunneling dielectric barriers had been achieved so successfully following the work of Giaever (1960).

By contrast, ASJ reflections have become a major tool for the study of unconventional superconductors, such as heavy fermions (Goll *et al.*, 1993; Hasselbach *et al.*, 1993), organic superconductors (see, for instance, Ernst *et al.*, 1994) and high-T_c superconductors, which are the focus of this review. This development is the object of this review. One of the reasons why we became involved in this field was that we had strong doubts that dielectric junctions of a quality comparable to that achieved by Giaever on low-temperature superconductors could ever be achieved on high-temperature superconductors. Dielectric junctions made on low-temperature superconductors are based on the oxidation of the metal. This method is not applicable to high-T_c superconductors, because they are oxides by themselves, and further oxidation renders them even more metallic (and eventually nonsuperconductors). Further, the fabrication of high-T_c superconductors requires high temperatures of the order of 700–800 °C and the use of single-crystal substrates, which precludes growing them on top of a regular metal previously oxidized. In our laboratory, we therefore decided to concentrate on the point-contact route. In fact, observation of ASJ reflections turned out to be relatively easy. I believe that Hass *et al.* (1992, 1993) were the first to report such observations on single-crystal high-quality YBCO samples, using a gold tip as the normal metal. For reasons that became clear only later and that had to do with the *d*-wave symmetry of the order parameter in this superconductor, the fit to Blonder-Tinkham-Klapwijk theory was not perfect, but a gap value of 18–20 meV could clearly be obtained. This value still stands today.

However, a determination of the energy gap is not the only, and may be not the most important, result of ASJ spectroscopy of high-T_c superconductor materials. The following points will give the reader a preliminary idea of the main results.

(a) A successful quantitative fit of point-contact data to the Blonder-Tinkham-Klapwijk theory, as has now been achieved in optimally doped samples, means that the Bogoliubov–de Gennes equations, or, in other words, a fermionic description of the excitations, is appropriate for high-T_c superconductors. ASJ reflections cannot occur without electron-hole mixing.

(b) According to Blonder and Tinkham (1983), an enhanced conductance below the gap is only possible if the Fermi velocities of the normal tip and of the superconductor are not too different. That this should be the case in high-T_c superconductor/normal-metal contacts is by no means trivial. In fact, angle-resolved photoemission spectroscopy (ARPES) data indicate for the high-T_c superconductor a Fermi velocity of the order of 2×10^7 cm/sec (Margaritondo, 1998), almost one order of magnitude smaller than that of gold. This apparent contradiction between experiment and theory was explained by Deutscher and Nozières (1994) as resulting from a renormalization of the Fermi velocity in the point-contact experiments, which is different from the full quasiparticle renormalization. This special renormalization also explains the occurrence of strong ASJ reflections in heavy fermions (Hasselbach *et al.*, 1993).

(c) The BCS approximation of an energy gap that is very much smaller than the Fermi energy applies extremely well to low-temperature superconductors, for which the gap value is typically less than 1 meV, and the Fermi energy value is several eV. It applies only marginally to the high-T_c superconductors at optimum doping, where the gap value is a few tens of meV and the Fermi energy value a few 100's of meV. It may not apply at all in underdoped samples, where a Bose-Einstein condensation regime could be approached. The properties of ASJ reflections in a regime that is intermediate between BCS and Bose-Einstein condensation (Leggett, 1980; Nozieres and Schmitt-Rink, 1985) are a subject of great current interest. In particular, the existence of ASJ reflections in the presence of preformed pairs (or, more generally, of a pairing amplitude) without phase coherence is under intense consideration.

(d) ASJ reflections are phase sensitive. This major difference from conventional Giaever tunneling spectroscopy turns out to be of great interest for the study of superconductors having an unconventional symmetry order parameter, as is the case for the high-T_c superconductors. As shown by Hu (1994), *d*-wave symmetry results in zero-energy surface bound states, or ASJ bound states, when the orientation of the surface with respect to the crystallographic axis is such that there are interference effects between ASJ reflections from lobes of the order parameter of opposite signs. This is in contrast with the finite-energy bound states calculated by de Gennes and Saint-James. The case of *p*-wave superconductors was earlier investigated by Buchholz and Zwicknagl (1981).

This review is organized as follows. In Sec. II, I briefly present the original calculation of de Gennes and Saint-James for a one-dimensional (1D) situation giving the finite energy of bound states in a normal slab in contact with a superconductor and contrast it with the zero-energy states obtained in a hypothetical situation in which the normal slab is sandwiched between two superconductors whose order parameters have phases that differ by π. This serves as an introduction to the effect of *d*-wave symmetry.

Section III is devoted to a brief summary of the Blonder-Tinkham-Klapwijk theory and to point-contact experiments in geometries where the *d*-wave symmetry plays only a minor role. These experiments lead to determinations of the gap and of a Fermi velocity that is different from the fully renormalized value. Renormalization of the latter as appropriate for point-contact spectroscopy is included in this section. Effects related to *d*-wave symmetry and, in particular, to the occurrence of surface bound states, are discussed in Sec. IV. This section includes the effect of surface currents on these

states. Section V is devoted to ASJ reflections in the underdoped or so-called pseudogap regime, in relation to a possible BCS-to-Bose-Einstein-condensation crossover and other pseudogap models. Other advanced topics, such as the occurrence and detection of a minority imaginary component (*is* or *id*) of the order parameter and the proximity effect between high-T_c superconductors and normal metals, are discussed in Sec. VI.

II. SOLUTION OF THE BOGOLIUBOV–de GENNES EQUATIONS NEAR AN N/S INTERFACE

In order to make this review self-contained, we shall briefly outline here the main steps of the derivation that can be found in detail in the article of Saint-James (1964).

We consider two metals in ideal contact, the only difference between them being that one is a superconductor and the other a normal metal. We concentrate on quasiparticle excitations having an energy ε measured from the Fermi level smaller than the energy gap Δ. Such excitations will necessarily decay in S. They do so over a certain length scale, which turns out to be on the order of the coherence length ξ of the superconductor. At larger distances from the interface, all electrons are paired. Thus the reflection process that we have briefly described in the introductory section, by which an electron coming from the N side is reflected as a hole, does not occur abruptly at the interface, but over the length scale ξ. This property, which appears explicitly in the calculation, will be of great importance when we discuss contacts with high-T_c superconductors, in particular in the so-called pseudogap region.

As it is, the calculation ignores the effect of the proximity of N on the value of the gap Δ in S near the interface. It is well known that this effect cannot, in general, be neglected and that a depression of Δ occurs over the length ξ (Deutscher and de Gennes, 1969). However, in the actual point-contact setup described by Blonder *et al.* (1982; see next section), the contact size is smaller than ξ so that this depression effect is much reduced and can be neglected.

A. The case of a normal slab in contact with a semi-infinite superconductor

In a normal metal, the excitation energies of electrons and holes are derived, respectively, from the following relations:

$$\varepsilon u = [-(\hbar^2/2m)\nabla - E_F]u, \tag{2.1}$$

$$\varepsilon v = [(\hbar^2/2m)\nabla + E_F]v. \tag{2.2}$$

In a superconductor, excitations have a mixed electron-hole character and the above equations are complemented by cross terms:

$$\varepsilon u = [-(\hbar^2/2m)\nabla - E_F]u + \Delta v, \tag{2.3}$$

$$\varepsilon v = [(\hbar^2/2m)\nabla + E_F]v + \Delta^* u. \tag{2.4}$$

The solutions for u and v are oscillatory in N, and for $\varepsilon < \Delta$ they are decaying in S with complex wave vectors. The conditions at the interface, assuming that it is perfectly transparent, are that u and v and their derivatives are continuous. At the outer surface of N, assumed to be bonded by a dielectric, the boundary conditions are that u and v are zero. With the normal slab having a thickness d_N, and taking the origin at the interface, one-dimensional solutions in N are of the form

$$u = \alpha \sin[k_1'(x + d_N)], \tag{2.5}$$

$$v = \beta \sin[k_2'(x + d_N)], \tag{2.6}$$

with

$$k_1' = [(2m/\hbar^2)(E_F + \varepsilon)]^{1/2}, \tag{2.7}$$

$$k_2' = [(2m/\hbar^2)(E_F - \varepsilon)]^{1/2}. \tag{2.8}$$

Solutions in S are of the form

$$u = \alpha_1 \exp(ik_1 x) + \alpha_2 \exp(-ik_2 x), \tag{2.9}$$

$$v = \beta_1 \exp(ik_1 x) + \beta_2 \exp(-ik_2 x). \tag{2.10}$$

The wave vectors are given by

$$k_1 = (2m/\hbar^2)^{1/2}[E_F + (\varepsilon^2 - \Delta^2)^{1/2}]^{1/2}, \tag{2.11}$$

$$k_2 = (2m/\hbar^2)^{1/2}[E_F - (\varepsilon^2 - \Delta^2)^{1/2}]^{1/2}. \tag{2.12}$$

Since we are interested in excitations for which $\varepsilon < \Delta$, these wave vectors are complex and their imaginary part ensures the exponential decay of the excitations inside S. We can write them in the form

$$k_1 = K_1 + iK_2, \tag{2.13}$$

$$k_2 = K_1 - iK_2. \tag{2.14}$$

To a good approximation, $K_1 = k_F$, and $K_2 \ll K_1$. It is instructive to calculate explicitly the decay wave vector. To fix the order of magnitude, we easily obtain it for $\varepsilon = 0$,

$$K_2(\varepsilon = 0) = \Delta/\hbar v_F, \tag{2.15}$$

which, except for a factor of π, is the inverse of the coherence length ξ. It can easily be seen that the decay length diverges when ε approaches Δ.

The ratios (β_1/α_1) and (β_2/α_2) are determined by the Bogoliubov–de Gennes equations, so that there are four unknowns and four homogeneous linear equations relating them (the boundary conditions at the interface). After some simplifications resulting form the fact that $(\Delta/E_F) \ll 1$, the condition for the existence of a solution to the eigenvalue problem reads

$$\tan(k_2' d_N) = \tan(k_1' d_N - \phi), \tag{2.16}$$

where ϕ is defined by

$$\Delta \cos\phi = \varepsilon. \tag{2.17}$$

Taking into account Eqs. (2.7) and (2.8), we find that the solutions of Eq. (2.16) are

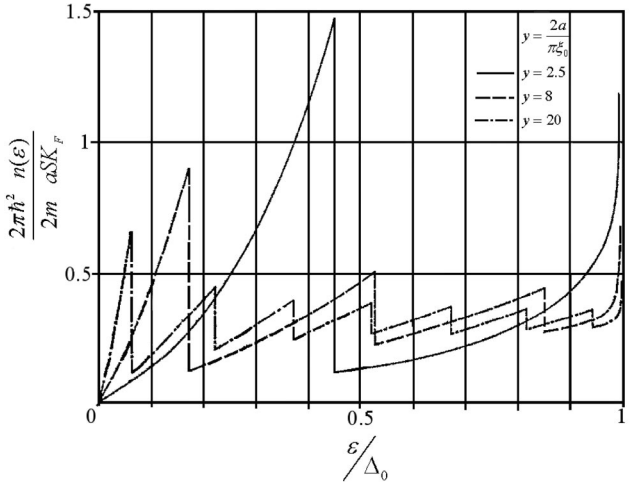

FIG. 1. Density of states for a normal-metal/superconductor (N/S) contact for different values of the normal layer thickness a. The thickness is given in terms of a normalized parameter $(2a/\pi\xi)$. Adapted from Saint-James, 1964.

$$(2d_N/\pi\xi)\cos\phi = \phi + n\pi, \tag{2.18}$$

where we have used the relation $\xi=(\hbar v_F/\pi\Delta)$. For any finite value of the normal slab thickness, there is no zero-energy solution. An energy gap has been induced in N by the proximity to S. When the slab thickness is small compared to the coherence length, there is only one solution at $\varepsilon<\Delta$ and it approaches Δ. This bound state is, in fact, localized over the length ξ, over which excitations can penetrate into S. When the thickness is much larger than ξ, ϕ approaches $\pi/2$. There are a large number of solutions, the separation between the levels being

$$\Delta\varepsilon = (\hbar^2/2m)(\pi k_F/d_N). \tag{2.19}$$

As noted by Saint-James (1964), this is half the spacing between the electronic levels in a 1D isolated normal metal of the same thickness. He explains this difference by noting that excitations in N in contact with S have a mixed electron-hole character. At energies smaller than Δ, the coefficients α and β are close to each other. Over a complete cycle comprising two ASJ reflections at the N/S interface and two specular reflections at the free surface of N, the quasiparticle is electronlike half of the time, and holelike the other half. This same Saint-James cycle leads, as we shall see, to the formation of zero-energy states at the surface of a d-wave superconductor.

In a more realistic 3D situation, instead of the discrete energy levels that we have obtained, the density of states is finite at any finite energy. Eigenvalues of the energy for quasiparticle trajectories making an angle Θ with the normal to the interface are reduced because the path traveled before the ASJ reflection takes place is longer. These eigenvalues tend to zero when Θ approaches $\pi/2$, but the solid angle covered by such trajectories tends itself to zero and as a result the density of states tends to zero linearly with ε (Fig. 1).

B. The case of a normal layer sandwiched between two superconductors: Effect of a phase difference

It follows from our analysis that we would have obtained the same eigenvalues if we had considered a normal slab of thickness $2d_N$ sandwiched between two superconductors. This is because, in that case, one reflection at each interface is sufficient to complete a cycle: an electron hitting the interface with S_1 is reflected as a hole, which is reflected back as an electron by S_2. As a matter of fact, this geometry was used to study the proximity effect by thermal conductivity measurements of S/N/S sandwiches (Wolf, 1971). These measurements did reveal a reduced density of states in N. But for what concerns us here, the main interest of an S/N/S geometry is that it allows us to look for the effect of a phase difference between the two superconductors on the density of states. Such a phase difference may, for instance, be induced by a current flowing perpendicular to the interfaces. To be specific, let us consider the case in which this phase difference is equal to π (this will be the case of interest for a d-wave superconductor). The pair potentials in S_1 and S_2 have then opposite signs. The Bogoliubov–de Gennes equations require that the ratios (u/v) also have opposite signs in S_1 and S_2. The continuity conditions at the interfaces then require that solutions in N be of the form

$$u = \alpha\sin[k_1'(x+d_N)], \tag{2.20}$$

$$v = \beta\cos[k_2'(x+d_N)]. \tag{2.21}$$

The solution to the eigenvalue problem is then

$$-\cot(k_2'd_N) = \tan(k_1'd_N - \phi), \tag{2.22}$$

$$(k_2'd_N) - \pi/2 = (k_1'd_N - \phi) + n\pi, \tag{2.23}$$

which gives the result

$$(2d_N/\pi\xi)\cos\phi = \pi/2 - \phi + n\pi. \tag{2.24}$$

In contrast to the case treated by Saint-James, it can immediately be seen that here $\phi=\pi/2$ is a solution for any value of the thickness. In other words, there exists a solution with the eigenvalue $\varepsilon=0$ even in the limit where the thickness of the normal slab is zero. In effect, one does not need a normal layer to obtain a zero-energy bound state when there is a change of phase by π. This zero-energy solution is localized near the interface between the two superconductors, and it decays in the superconducting banks over a coherence length. It is a zero-energy interface bound state. A self-consistent solution would, of course, give a pair potential going to zero at the interface. The situation is similar to that near a vortex core: on opposite sides of the core, phases differ by π, the pair potential goes to zero at the center of the vortex core to accommodate this change in the phase, and there are low-lying states of extension ξ (Caroli *et al.*, 1964).

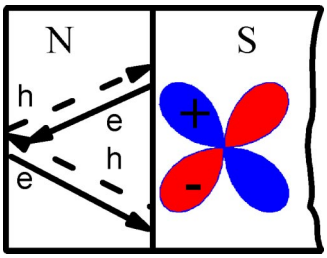

FIG. 2. (Color in online edition) Schematic representation of an Andreev–Saint-James (ASJ) cycle for a *d*-wave superconductor coated with a normal-metal layer, the interface being oriented perpendicular to a nodal direction.

C. Surface bound states in a *d*-wave superconductor

The situation described in the previous subsection is somewhat artificial, particularly in the limit of a zero-thickness normal slab. But this exercise helps us to understand what happens at the surface of a *d*-wave superconductor when it is oriented perpendicular to a node direction. For the $d_{x^2-y^2}$ symmetry, the pair potential is of the form

$$\Delta = \Delta_0 \cos 2\theta, \tag{2.25}$$

where θ is the angle with one of the principal axes (the antinodal direction). The pair potential is at a maximum along these axes and changes signs at 45° from them (the nodal direction). The pair potentials on either side of these nodes have the same absolute values, but opposite signs. Let us go back to the original Saint-James geometry and consider a normal-metal slab in contact with the surface of a *d*-wave superconductor having the above orientation (Fig. 2). An electron in N moving towards the interface with a wave vector at some finite angle with the interface will be ASJ reflected as a hole by a pair potential having, say, positive sign. This hole will then be specularly reflected at the outer surface of N, after which it will be ASJ reflected as an electron by a pair potential having negative sign. This electron will then, in turn, be specularly reflected at the free surface of N, which will close the Saint-James cycle. This process is equivalent to that treated in the above subsection: there are two successive ASJ reflections by pair potentials having phases that differ by π. Zero-energy states are formed in N and extend inside S over a coherence length. This geometry was first studied by Hu (1994), who showed that zero-energy states are formed even in the limit of a zero-thickness normal slab, as in the above exercise. In the semiclassical approximation, they are zero-energy surface bound states, or ASJ bound states.

The spectroscopic study of these states will constitute a substantial part of this review. Whenever detected, they are a clear signature of a pair potential that reverses sign around the Fermi surface. They are modified by the presence of even a small imaginary component, such as *is* or id_{xy}, which cancels the sign reversal in the vicinity of a *d*-wave node. In this way, such components can be detected and their amplitude measured. In short, the spectroscopic study of ASJ states allows the determination of the detailed symmetry of the pair potential and the respective amplitudes of its components.

It will be appreciated that ASJ bound states will be best studied by tunneling from a normal-metal electrode through a junction formed directly at the surface of the *d*-wave superconductor having the appropriate orientation. Making a clean contact with a normal metal would result in short-lived ASJ states.

ASJ spectroscopy of the high-T_c superconductors thus employs two different contact techniques: (1) clean Sharvin contacts are appropriate when formed on surfaces oriented perpendicular to an axis along which the order parameter is at its maximum, because in that geometry no ASJ bound states are formed and the amplitude of the gap is immediately accessible; (2) tunneling contacts are preferred when formed on surfaces oriented perpendicular to a (presumed) node direction, in order to detect the presence of ASJ bound states due to an unconventional order-parameter symmetry. These two methods are reviewed in the following sections.

III. CONDUCTANCE CHARACTERISTICS OF SHARVIN CONTACTS

A. Sharvin contacts as a tool for ASJ spectroscopy

Let us consider a clean contact between two metals having a very small cross section a^2, so that its electrical conductance in the normal state is equal to the number of quantum channels connecting them, multiplied by the quantum conductance $(e^2/\hbar)$. We neglect for the time being any resistance that might arise from a dielectric barrier between the two metals, or from a mismatch of the Fermi velocities between them. Such a situation can be nearly realized if we use broad-conduction-band metals, since they all have Fermi velocities of the order of 1×10^8 cm/sec, and if we can avoid the formation of an oxide at the interface. The current-voltage relationship of this contact is

$$I = (e^2/h)(k_F a)^2 V. \tag{3.1}$$

The current density through the contact is

$$J = nev, \tag{3.2}$$

where n is the carrier density and v is the velocity across the contact. From Eq. (3.1) and the current-density definition $J=(I/a^2)$, we obtain for the velocity the expression

$$v = (eV/h)(k_F^2/n). \tag{3.3}$$

When we use Sharvin contacts to perform ASJ spectroscopy, the bias across the contact will reach values of the order of the pair potential. Using the value for the carrier density in the free-electron model, we obtain at such bias a velocity of the order of

$$v = (\Delta/p_F), \tag{3.4}$$

which is the depairing velocity in the superconducting side with gap Δ.

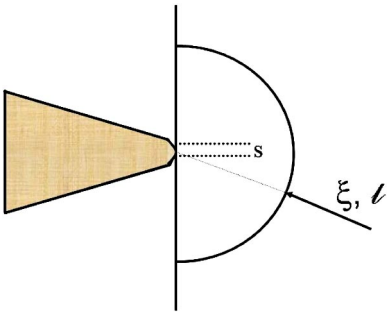

FIG. 3. (Color in online edition) Schematic representation of a Sharvin point contact having a size s much smaller than the coherence length ξ and the mean free path l. At biases of the order of the gap, the current density at the contact is of the order of the depairing value, but at distances of the order of (ξ,l), it is reduced much below that value. The condition $s \ll (\xi,l)$ avoids heating effects and quenching of superconductivity in the vicinity of the contact.

This high velocity is the main reason why we must use a contact size both smaller than the electron mean free path—in order to avoid heating effects—and smaller than the coherence length (Fig. 3). Spreading of the current after the contact bottleneck then reduces the current density below the depairing value even at distances smaller than ξ, thus avoiding quenching superconductivity at the contact, since superconductivity cannot be quenched over a length scale smaller than ξ.

In summary, a small contact size is favorable for three reasons: (i) the condition $a \ll l$ makes the contact ballistic, which prevents heating effects at the large current densities reached at biases of the order of the gap; (ii) the condition $a < \xi$ plays two roles: it prevents the weakening of superconductivity in S due to the proximity with N; and it prevents the destruction of superconductivity at biases of the order of the gap, where the carrier velocity reaches the depairing value (Δ/p_F).

B. Fabrication of Sharvin contacts

In a clean superconductor the mean free path $l > \xi$, and the above conditions are met if $a < \xi$. In a low-temperature superconductor, ξ is typically of the order of 1000 Å, and the contact qualifies as a Sharvin contact if $a \approx 100$ Å. For a high-T_c superconductor, we would rather require $a \approx 10$ Å. When making a point contact, how can we make sure that such conditions are met?

The fabrication of point contacts has been well described in the literature; see, for instance, Blonder *et al.* (1982). In short, a relatively sharp metallic tip, having a local radius of curvature of the order of 1 μm, is brought delicately into contact by a mechanical device with a bulk counterelectrode. The tip can be, for instance, made of a thin gold wire, cut with a sharp razor blade. If the actual size of the contact were of the order of the radius of curvature of the tip, the above conditions would not be met. Its electrical resistance would be of the order of 1 mΩ. In fact, the resistance of the contact is often found to be of the order of 10–100 Ω. But how can we determine whether this larger value actually reflects a small contact size, or rather a dirty contact? We can get an answer to this question if we combine the value of the normal-state resistance R_N (namely, its value above the critical temperature, or more practically its value well above the gap bias) with its value R_S at low bias (below the gap). In an ideal contact, we would have $(R_N/R_S)=2$. This is, of course, never achieved. But a ratio $(R_N/R_S)>1$ is an indication that ASJ reflections may dominate, although some junction structures (such as a proximity effect across the junction) may give such ratios and should be carefully checked, for instance, through the bias dependence of the conductance.

It turns out that in many cases the contact realized is indeed clean, and its size falls in the range of a few tens of angstroms. One may wonder how that can happen, in view of the rather crude contact technique used here. As practitioners know from experience, when the tip is first brought into contact with the counterelectrode, the resistance is usually fairly high, in the range of a few kΩ, and the $I(V)$ characteristic is structureless. By applying some slight movements to the tip, however, it is, possible to bring the resistance down to the interesting range of 10–100 Ω and to obtain meaningful characteristics. One may conjecture that these movements scratch away some of the insulating material at the surface, revealing the underlying pristine material. This, however, does not explain the very small size of the contact achieved. On the other hand, it is well known that when trying to produce a uniform tunneling barrier, one often encounters a problem of shorts, presumably due to pinholes in the barrier. It may be that small good contacts are established through some naturally occurring defects in the insulating layer, but this is still imperfectly understood. Small-size contacts have been observed using very different techniques of tip preparation, such as electrochemical etching of a Nb wire, or cutting a thin Au wire with a sharp razor blade, as said before. These methods of tip preparation were reviewed by Achsaf *et al.*, 1996.

C. Blonder-Tinkham-Klapwijk model

An electron moving from the N side towards the interface can be scattered in four different ways:

(i) it can be reflected as a hole along the incident trajectory (ASJ reflection) with probability $A(\varepsilon)$;

(ii) it can be reflected as an electron (normal specular reflection) with probability $B(\varepsilon)$;

(iii) it can be transmitted as an electron having a momentum $k > k_F$ (no branch crossing) with probability $C(\varepsilon)$;

(iv) it can be transmitted as an electron having a momentum $k < k_F$ (branch crossing) with probability $D(\varepsilon)$.

The sum of these probabilities must be equal to 1:

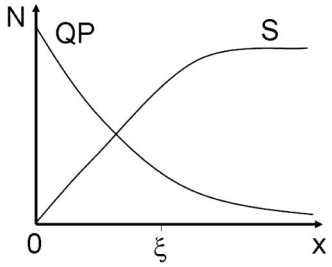

FIG. 4. Buildup of the superfluid density S and decrease of the quasiparticle density QP in the superconductor side of an N/S contact. ASJ reflections build up progressively over the distance ξ.

$$A(\varepsilon) + B(\varepsilon) + C(\varepsilon) + D(\varepsilon) = 1. \tag{3.5}$$

Since current is conserved across the interface, it suffices to calculate it, for instance, at the N side of the contact:

$$I = J_0 \int_{-\infty}^{+\infty} [1 + A(\varepsilon) - B(\varepsilon)][f(\varepsilon - eV) - f(\varepsilon) d\varepsilon, \tag{3.6}$$

where $f(\varepsilon)$ is the Fermi function and J_0 is a conductance taking into account the geometry of the contact.

Blonder *et al.* (1982) have given a complete calculation of the dependence of coefficients A and B on energy for barriers characterized by a delta-function potential. For their derivation, we refer the reader to their paper. Here, we limit ourselves to some simple limiting behaviors that we feel are of particular importance.

1. Case of a clean interface

For a clean interface, there are no specular reflections at the interface, $B(\varepsilon)=0$. Also, $A(\varepsilon)=1$ for $\varepsilon<\Delta$. For $\varepsilon>\Delta$, excitations can propagate in S. They have a partial electron character with amplitude u_0, and a partial hole character with amplitude v_0. From BCS theory, we know that

$$u_0^2 = [1 + (\varepsilon^2 - \Delta^2)^{1/2}/\varepsilon]/2, \tag{3.7}$$

$$v_0^2 = [1 - (\varepsilon^2 - \Delta^2)^{1/2}/\varepsilon]/2. \tag{3.8}$$

ASJ reflections occur in proportion to the probabilities for a hole-to-electron character of the excitations propagating in S:

$$A(\varepsilon) = [1 - (\varepsilon^2 - \Delta^2)^{1/2}/\varepsilon]/[1 + (\varepsilon^2 - \Delta^2)^{1/2}/\varepsilon]. \tag{3.9}$$

The conductance is equal to twice the normal-state value below the gap and goes back to it over a scale Δ in a manner that can be calculated from Eqs. (3.9) and (3.6).

It is interesting to consider more closely how the normal current in N is converted into a superfluid pair current in S (Fig. 4). As already shown by Saint-James, and noted earlier in this review, there are evanescent quasiparticle waves in S at excitation energies smaller than the gap. They decay over a length scale of the order of ξ, and are at the same time converted into a superfluid. More precisely, Blonder *et al.* (1982) show that the decay length is given by

$$\lambda = (\hbar v_F/2\Delta)[1 - (\varepsilon/\Delta)^2]^{-1/2}. \tag{3.10}$$

This progressive conversion of quasiparticles into a superfluid has important consequences, some of which we have already outlined. At a distance ξ from the interface, the current density is reduced by a factor of $(a/\xi)^3$, which, in a low-temperature superconductor, can be a factor of 1×10^{-6}. The velocity is then negligible compared to the depairing velocity, even at biases much larger than the gap. The situation is plainly much less favorable in a high-T_c superconductor because of the short coherence length. Thus we can hope at small bias to have, at best, $a \leqslant \xi$. However, as the bias is increased, the situation becomes more favorable because of the divergence of the decay length. Another point, which is trivial for low-temperature superconductors, is that propagation of quasiparticles over a distance ξ from the interface is necessary for the conversion to take place, and therefore for full ASJ reflections to occur. This condition is not a trivial one when we consider some situations peculiar to the high-T_c superconductors, such as the existence of a pseudogap that may be larger than the pair potential. This special situation will be discussed in a later section.

2. Contacts with a finite transparency

Blonder *et al.* (1982) calculated the coefficients $A(\varepsilon)$ and $B(\varepsilon)$ for contacts with a finite transparency, which they modeled with a δ-function barrier $V=H\delta(x)$. They used in their calculation a dimensionless parameter $Z=(H/\hbar v_F)$. For the case in which the Fermi velocities in N and S are different, Blonder and Tinkham (1983) showed that one can replace Z by an effective barrier parameter,

$$Z_{\text{eff}} = Z^2 + (1 - r)^2/4r^2, \tag{3.11}$$

where $r=v_{FN}/v_{FS}$ (or the inverse). The shape of the $I(V)$ characteristics is a function of Z_{eff} only. There is no way one can distinguish between the effects of a dielectric barrier and that of a mismatch between the Fermi velocities. This result, obtained for a delta-function barrier, is not general. In particular, it does not hold when the normal side is spin polarized (see the last section of this review).

A finite Z results in a finite probability of ordinary specular electron reflections at the N/S interface. $B(\varepsilon)$ is now finite, $A(\varepsilon)<1$ even at $\varepsilon<\Delta$: the conductance below the gap is smaller than $2R_N^{-1}$; it goes to zero as Z is made very large. Blonder *et al.* (1982) showed that, at zero bias,

$$A(0) = (1 + 2Z_{\text{eff}}^2)^{-2}. \tag{3.12}$$

Since at biases smaller than the gap $C=D=0$, it follows from the sum rule $A+B+C+D=1$ and from Eq. (3.6) that the current at zero bias is proportional to $2A(0)$. In

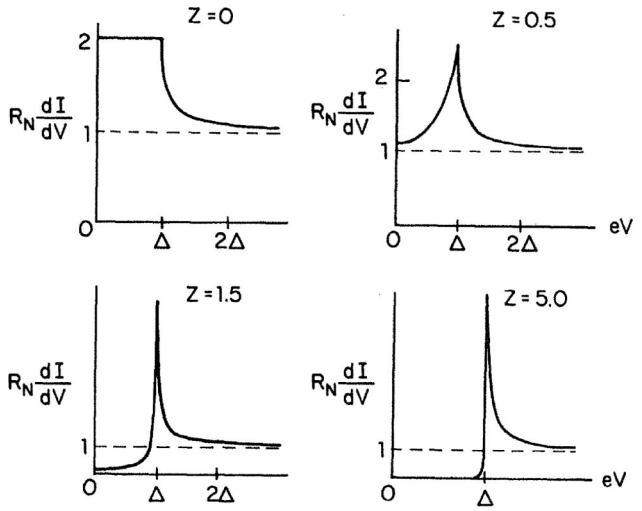

FIG. 5. Conductance characteristics of N/S contacts for various values of the barrier parameter Z. Adapted from Blonder *et al.*, 1982.

the normal state, or at a bias much larger than the gap, it is proportional to $(1-B)=(1+Z_{\rm eff}^2)^{-1}$. From Eq. (3.5), the ratio of the zero-bias to the high-bias resistances, (R_S/R_N), is thus given by

$$(R_S/R_N) = 2(1+Z_{\rm eff}^2)/(1+2Z_{\rm eff}^2)^2. \tag{3.13}$$

From the measurement of the ratio of the contact resistances at high and zero bias, one can calculate the value of the effective barrier parameter. This value is useful for two purposes. First, it allows the calculation of the actual size of the contact by

$$(k_F a)^2 = (h/R_N e^2)(1+Z_{\rm eff}^2). \tag{3.14}$$

Second, this parameter gives a lower bound on the ratio of the Fermi velocities by assuming the absence of any dielectric barrier at the interface.

More generally, using the analytical expressions derived by Blonder *et al.* (1982) for the coefficients $A(\varepsilon)$ and $B(\varepsilon)$, it is possible to fit experimental $I(V)$ curves and to extract values of the gap and of the barrier parameter. Figure 5 gives a few examples of conductance characteristics calculated for different values of the barrier parameter. As it increases, the normalized zero-bias conductance falls below 2, while at the gap edge it increases above 2. In fact, at the gap edge the conductance value is unaffected by the barrier. Blonder *et al.* (1982) obtained values of the gap and of the Z parameter by fitting the conductance curves of Nb/Cu Sharvin contacts to their theory (see Blonder and Tinkham, 1983). Characteristics could be fitted successfully for normal-state resistances falling in the range of 10–100 Ω. Reported values of $Z_{\rm eff}$ were smaller than 1, and could be as small as 0.3. Calculated contact radii varied from 10 to 120 Å, fully qualifying them as Sharvin contacts meeting the conditions $a<(\xi,l)$. The bound to the mismatch of the Fermi velocities was as expected. In fact, the experimentally determined values of the effective barrier parameter mean that the contact was basically a clean one. In turn, this justified modeling the barrier as a δ function, since the mismatch of the Fermi velocities occurred over an atomic distance.

D. High-temperature superconductor point-contact results for an antinodal orientation

1. Early experiments on high-quality single-crystal YBCO samples

The earlier Sharvin point-contact experiments on high-quality single-crystal samples were performed by Hass *et al.* (1992) on melt-textured YBCO samples cut out in a cubic shape so that four faces had the (100) or equivalent orientation and two the (001) orientation. As already noted, the main motivation for attempting this experiment was the hope that there was a better chance of obtaining a good point contact than of making a good tunnel junction. Hass *et al.* revealed the following main features.

(a) On the (100) faces, contacts with a normal-state resistance of about 10 Ω could be made. Their conductance increased by about 50% below a bias of about 20 mV (Fig. 6). This bias value was interpreted as being the gap edge. The shape of the characteristic was generally in accordance with the predictions of Blonder *et al.* (1982) for a barrier parameter of about 0.3, except for two features. First, the return to the normal-state conductance above the gap was somewhat faster than it should have been; this might have been due to the fact that the condition $a<\xi$ was only barely met, because of the short coherence length. Second, the data did not show the expected conductance peak at the gap edge. The absence of this conductance peak was also noted later on similar contacts produced on LSCO samples (Hass *et al.*, 1994). The main surprise came from the substantial enhancement of the conductance at low bias, which implied a small mismatch of the Fermi velocities.

(b) On the (001)-oriented faces, the characteristics were basically structureless except for an occasional zero-bias peak, and positive slopes at negative as well as positive biases. The absence of a conductance enhancement at low bias for this orientation was expected, in view of the large mismatch of the Fermi velocities for that case. However, Blonder-Tinkham-Klapwijk theory then predicts that the characteristic should have the shape of a regular Giaever tunneling junction, which was not observed.

2. Effect of *d*-wave symmetry for an antinodal direction

The original theory of Blonder *et al.* (1982) is not appropriate for d-wave symmetry. However, the later version does not have dramatic effects for an antinodal direction, probed in the experiments of Hass *et al.* (1992). As noted above, there are no ASJ low-energy surface bound states for that orientation because specular reflections at the surface then preserve the value and the sign of the pair potential. The coefficients A and B can be calculated by performing a 2D integral of the Blonder-Tinkham-Klapwijk coefficients over all angles.

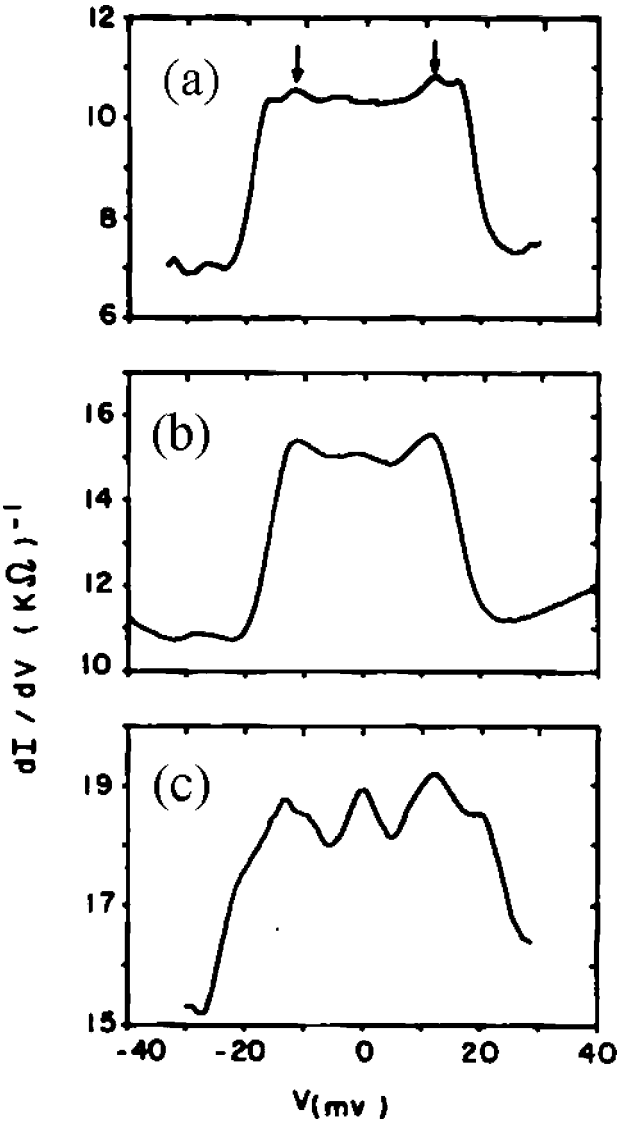

FIG. 6. Conductance characteristics of Au/YBCO point contacts for the antinodal orientation. The increase in the conductance at low bias is about 50%. The edge is at about 20 mV. Note the absence of a conductance peak at the gap edge. Data from three different locations on the same sample. Adapted from Hass *et al.*, 1992.

For clean contacts, having an effective Z parameter smaller than 1, it is not necessary to take into account a finite tunneling cone aperture. Typical shapes of conductance characteristics are shown in Fig. 7 (Z values: 0; 0.2; 0.3; 0.5; 0.7; 1.0). For $Z=0$, they assume a triangular shape; for Z values around 0.3, they are rather flat up to the gap edge, which is the case observed in the early experiments on YBCO shown above; for Z values in the range of 0.5–1, they assume a V shape at low bias, reaching a maximum slightly below the gap, followed by a sharp descent back to the normal-state conductance. We note that for an antinodal direction in this range of Z values, which is typical for point contacts, the maximum conductance reached is always smaller than twice the normal-state value. Typical maximum conductance values are around 30–50 % higher than the normal-state value.

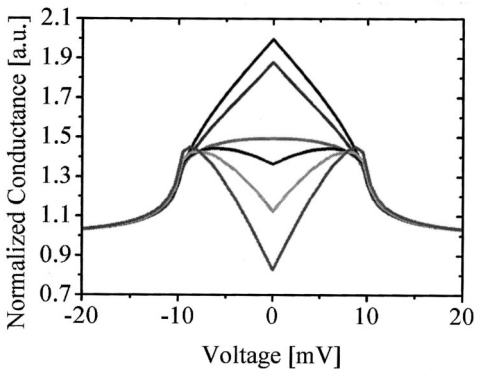

FIG. 7. Calculated conductance characteristics for a d-wave order parameter in an antinodal orientation, at different values of the barrier parameter Z (0; 0.2; 0.3; 0.5; 0.7; 1.0). Note for $Z>0.5$ the clear V shape at low bias and the sharp decrease in the conductance at the gap edge.

The d-wave symmetry explains the main disagreement between the data of Hass *et al.* (1992) and the original Blonder-Tinkham-Klapwijk theory, namely, a conductance at the gap edge smaller than twice the normal-state value. Actually, the various theoretical shapes calculated for the range $0<Z<1$ have been observed experimentally. Figure 8 shows data obtained on an a-axis-oriented YBCO surface (Kohen *et al.*, 2003), and Fig. 9 shows data obtained on a BiSrCaCuO single crystal in the (100) orientation (D'Gorno and Kohen, 1998), with fits to theory. The predicted V shape at low bias is clearly observed in both cases. Fits are of a high quality and require only a small "smearing" factor Γ (Kohen *et al.*, 2003). Kohen *et al.* establish that ASJ spectroscopy is a reliable and quantitative spectroscopic tool for the study of high-T_c superconductors. When performed in an antinodal direction, it provides a precise determination of the gap value. The effect of the d-wave symmetry can be clearly seen in the shape of the characteristics.

Two kinds of deviation from pure d-wave behavior have been reported. A special proximity effect has been observed between the normal tip and the d-wave superconductor at very small Z values ($Z<0.5$), which may induce an *is* component in the superconductor. This is discussed in detail in the last section of this review. Another deviation has been seen in strongly overdoped YBCO samples. It involves a small imaginary minority component (id_{xy} or *is*), whose occurrence is also discussed in the last section.

E. Renormalization of the Fermi velocity

1. The problem of the small Fermi velocity mismatch

The other question raised by the experiments of Hass *et al.* (1992) was the surprisingly small value of the barrier parameter needed to fit some of the data. Z values of 0.3–0.4, as found for YBCO (Hass *et al.*, 1992; Wei *et al.*, 1998) imply that the ratio between the Fermi veloci-

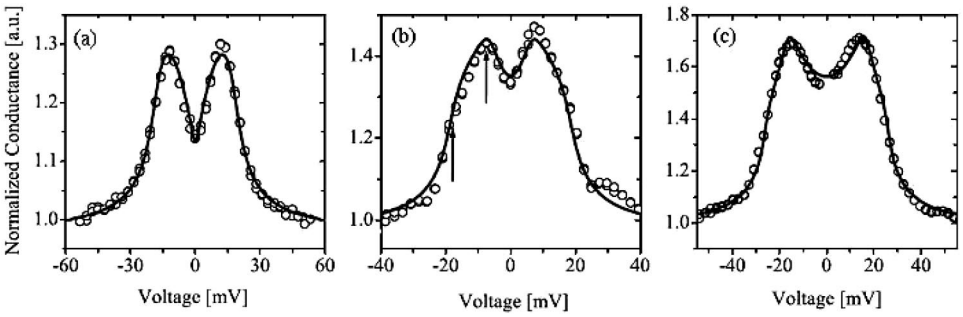

FIG. 8. (Color in online edition) Conductance characteristics of Au/YBCO film contacts fitted to a d-wave order parameter for different values of the barrier parameter Z (from left to right: 0.68; 0.49; 0.34). The fit is for an antinodal direction. Note the pronounced V shape at low bias for the highest-Z contact. Adapted from Kohen *et al.*, 2003.

ties of YBCO and of the normal tip is, at most, a factor of 2 (assuming that the finite Z is entirely due to the Fermi velocity mismatch). Taking, for instance, the case of the Au tip, in which the Fermi velocity is 1.4×10^8 cm/sec, one obtains for the Fermi velocity in YBCO a lower bound of 0.7×10^7 cm/sec. This is more than three times larger than the velocity measured by ARPES in BiSrCaCuO, $v_{FS}=2\times10^7$ cm/sec (see, for instance, Margaritondo, 1998), which is presumably typical of all high-T_c superconductors. Using this value of v_{FS}, one obtains $Z=6$. For such a high Z value, the point-contact characteristic should be a tunneling one (Tanaka, 1996), that is, the small-bias conductance should be much smaller than the normal-state value, contrary to what is observed experimentally.

2. Solution to the problem

As shown by Deutscher and Nozières (1994), the solution to the problem lies in the fact that the small value of the quasiparticle Fermi velocity in the cuprates is a many-body effect, which does not come into play in the mismatch that governs ASJ reflections. The quasiparticle velocity is

$$v_F = z\bar{v}_F, \tag{3.15}$$

where

$$\bar{v}_F = v_{F0} - \partial\Sigma/\partial k \tag{3.16}$$

and

$$z = 1/(1+\partial\Sigma/\partial\omega). \tag{3.17}$$

Here v_{F0} is the bare Fermi velocity (the band velocity, undressed for interaction effects), and Σ is the self-energy correction $\Sigma(k,w)$. The wave-vector dependence of the self-energy is a nonlocal effect (usually quite small in metals), and its energy dependence is a retardation effect, leading to mass enhancement. This factor can sometimes be extremely large, as in heavy fermions (Hasselbach *et al.*, 1993). It is, in principle, accessible by a measurement of the low-temperature electronic heat capacity. In practice, however, that is not possible in the high-T_c cuprates, because of their extremely high critical field. Another quantity that is sensitive to the mass enhancement factor is the coherence length, since it is the quasiparticle velocity that enters into that length:

$$\xi = \hbar v_F/\pi\Delta, \tag{3.18}$$

where Δ is the measured gap. We can obtain the value of v_F from Eq. (3.17), putting in the value of ξ derived from the measured upper critical field $Hc_2=\phi_0/2\pi\xi^2$, and the value of Δ obtained, for instance, from ASJ spectroscopy, as described in the previous paragraph. We can then calculate the mass-enhancement factor z by comparing this value of v_F to the lower bound of the velocity obtained from the effective barrier parameter $Z_{\rm eff}$ determined from a fit to point-contact conductance characteristics.

If we take the specific example of YBCO, from $\xi=15$ Å, $\Delta=20$ meV, we calculate for the quasiparticle velocity $v_F=1.5\times10^7$ cm/sec. The lower bound of the velocity obtained from the lowest measured $Z_{\rm eff}=0.3$ is, from Hass *et al.* (1992), $6–7\times10^7$ cm/sec, giving a mass enhancement factor of 4–5. It should be emphasized that this factor combines two effects: nonlocality and retar-

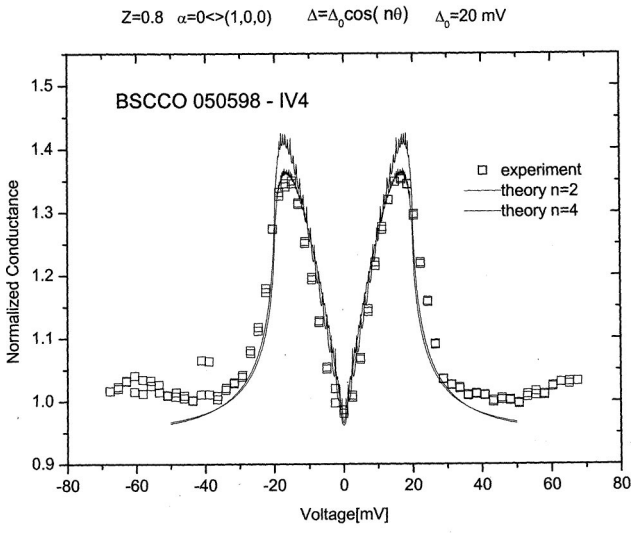

FIG. 9. Measured conductance characteristic of a $Au/Bi_2Sr_2CaCu_2O_8$ in-plane contact to a bulk-oriented sample. Note the low-bias V shape and the sharp drop at about 20 mV. The fit is for an antinodal direction and $Z=0.8$. Adapted from Okashi and Kohen, 2002.

dation. The respective contributions of these two effects cannot be determined directly. This would require a fairly exact knowledge of the bare-band velocity. Massida *et al.* (1991) showed that it is smaller than the velocity derived from the point-contact measurements, suggesting that both contributions are important.

F. Summary

In this section, we have reviewed the application of the Blonder-Tinkham-Klapwijk model to the study of ASJ reflections. We have shown that it can be applied successfully, in a quantitative way, to point-contact experiments carried out on high-T_c superconductors in configurations where phase effects due to the *d*-wave symmetry of the order parameter are not dominant. The Blonder-Tinkham-Klapwijk model is based on a solution of the Bogoliubov–de Gennes equations for the pair potential. Use of these equations implicitly assumes a Fermi-liquid description of the superconductor. The high quality of the fit between experiment and theory shows that this assumption is justified, at least for samples near optimum doping. The exact shape of the point-contact conductance characteristics obtained on surfaces perpendicular to an antinodal direction is in excellent agreement with a *d*-wave order parameter. The small value of the barrier parameter Z implies a good match between the Fermi velocities of the normal-metal tip and the high-T_c superconductor, which is well explained by a mass enhancement effect in the spirit of Fermi-liquid theory.

Geometries in which the *d*-wave symmetry has a more dramatic effect are reviewed in the next section.

IV. ASJ SURFACE BOUND STATES

As was briefly mentioned in Sec. II.C, zero-energy ASJ surface bound states are a direct result of a *d*-wave symmetry of the order parameter when the surface is oriented perpendicular to a nodal direction [(1,1,0)-oriented surface]. The origin of these states lies in the sign reversal of the pair potential "seen" by quasiparticles upon specular reflection at the surface. For reasons of symmetry, sign reversal for this orientation will occur for trajectories making any angle with the normal to the surface. For other surface orientations, sign reversal will occur for a certain angular range, with the exception of the case of the antinodal orientation, reviewed in Sec. III.D, where there is no sign reversal for any trajectory. Hence zero-energy surface bound states will exist for any surface orientation except the antinodal one. In the (more practical) case of diffuse reflections at the surface, for any orientation of the surface there will always be a sign reversal for some trajectories. Surface bound states are therefore a robust property of *d*-wave superconductivity.

A. Zero-bias conductance peaks and *d*-wave symmetry

Motivated by the findings of Hu (1994), Kashiwaya *et al.* (1995; Tanaka and Kashwaya, 1995) have extended the model of Blonder *et al.* to the case of a *d*-wave symmetry for all surface orientations.

The main difference from the results of Blonder *et al.* (1982), obtained for the *s*-wave symmetry case, comes about when one considers the two transmission channels having the respective transmission probabilities $C(\varepsilon)$, for an electronlike transmission, and $D(\varepsilon)$ for a holelike transmission. While in the *s*-wave case a 1D calculation was sufficient, automatically taking care of momentum conservation in the direction parallel to the interface, here a 2D calculation is necessary. A complete review of the theory and early experiments has been given by Kashiwaya and Tanaka (2000).

1. Results of Kashiwaya *et al.* for the (110) orientation

We summarize here the results of Kashiwaya *et al.* (1995) for the nodal orientation, following their notation and defining a normalized conductance as

$$\sigma(\varepsilon) = \bar{\sigma}_S(\varepsilon)/\bar{\sigma}_N(\varepsilon), \tag{4.1}$$

where

$$\bar{\sigma}_i(\varepsilon) = \int_{-\pi/2}^{+\pi/2} \bar{\sigma}_i(\varepsilon,\phi)d\phi \quad (i = N,S), \tag{4.2}$$

ϕ being the angle with the normal to the surface.

In the limit $Z \gg 1$, this expression reduces to

$$\bar{\sigma}_N(\varepsilon,\phi) = 4\cos^2\phi/Z^2, \tag{4.3}$$

$$\bar{\sigma}_S(\varepsilon,\phi) = 32\cos^4\phi/|4\cos^2\phi + Z^2(1+\Gamma^2)|^2 \tag{4.4}$$

with

$$\Gamma = \varepsilon/|\Delta| - [(\varepsilon/\Delta)^2 - 1]^{1/2}. \tag{4.5}$$

At zero bias, we have just $\sigma_S(0,\phi)=2$. The conductance is twice as large as the value it would have in the normal state in the absence of any barrier (Deutscher and Maynard, 1998). On the other hand, the actual normal-state conductance varies as Z^{-2}. Hence the appearance in the measured conductance of what is called a zero-bias conductance peak for a high-barrier contact. The bias range over which the conductance is substantially enhanced compared to its actual normal-state value is

$$|\varepsilon/\Delta| \leqslant Z^{-2}. \tag{4.6}$$

As the barrier height is increased, the conductance peak becomes higher and narrower. Lifetime effects and discrete lattice effects on the zero-bias conductance peak have been discussed by Walker and Pairor (1999). They broaden and reduce the zero-bias conductance peak. Discrete lattice effects limit zero-energy bound states to certain orientations of the wave vector. They can also modify the shape of the conductance peak near zero bias. There can thus be substantial deviations from the Kashiwaya *et al.* (1995) expressions. Since the conduc-

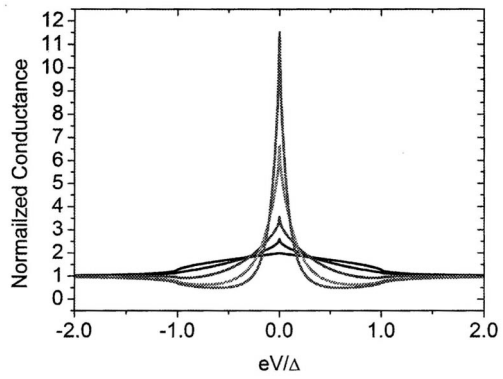

FIG. 10. Calculated conductance characteristics for a contact to a d-wave superconductor in a nodal direction, for different values of the barrier parameter Z (0; 0.5; 1.0; 2.0; 3.0). Contrary to the case of antinodal contacts, there is no sharp structure at the gap bias, only a smooth return to the normal-state conductance.

tance at zero bias $G_S(0)$ is unaffected by the presence of a barrier for a pure (110) orientation, its value may be used to calculate the actual size of the contact:

$$(k_F a)^2 = (\hbar/e^2) G_S(0). \tag{4.7}$$

Figure 10 shows how the shape of the conductance characteristic evolves as a function of Z for the (110) orientation. For $Z=0$, it has a triangular form, the conductance at zero bias being twice as large as the normal-state value, reached when the applied bias is equal to the value of the gap. For $Z \gg 1$, the conductance dips below its normal-state value before returning to it at a bias of the order of the gap. Notice that the gap is not marked by a sharp structure at any value of Z. Hence the (110) orientation is not as favorable as the (100) one for an accurate determination of the gap. On the other hand, it is highly sensitive to the symmetry of the order parameter.

2. Results of Kashiwaya *et al.* for arbitrary orientations

Kashiwaya *et al.* (1995) have given expressions for the amplitudes of hole $a(\varepsilon, \phi)$ and electron $b(\varepsilon, \phi)$ reflections. These expressions allow us to calculate the $I(V)$ characteristics for any surface orientation and Z value, taking into account a possible angular dependence of Z in the case of a strong barrier (tunneling cone). The zero-bias conductance peak is a robust feature of d-wave symmetry (Fig. 11; Yang and Hu, 1994). It occurs for any orientation of the surface except the (100) one, and for any value of Z. The structure at the gap edge is, in general, a weak one. It can be a small step down at low Z values, a small step up at large Z values, or a weak maximum at large Z values and intermediate orientations. An important difference between a contact and an s-wave superconductor is that no large conductance peak is predicted at the gap edge [even for the (100) orientation it remains of modest height]. This peak, called the coherence peak in s-wave superconductors, is

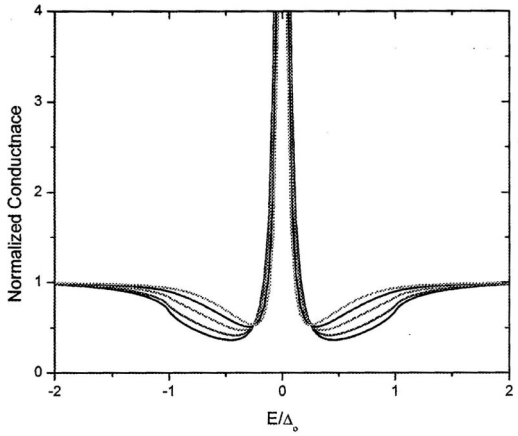

FIG. 11. Calculated conductance characteristics for a contact to a d-wave superconductor in a nodal direction with $Z=5$, at different openings of the tunneling cone. Return to the normal-state conductance always occurs at about the gap value. The curves have been calculated using the weight function $\exp[-(\theta/\theta_M)^2]$, with θ_M values 90°, 57°, 33°, 23°, and 18°.

destroyed for in-plane tunneling by the very interference effects that give rise to the zero-bias conductance peak.

B. Experimental results

We review in turn results obtained for low-Z contacts (Sharvin contacts) and high-Z contacts (tunneling contacts).

1. Low-Z (110) contacts

Figure 12 shows the conductance of a contact prepared on a (110) face of a LSCO single crystal (Dagan *et al.*, 2000). The crystal itself had $T_c=33$ K, near optimum doping, but the local T_c at the contact was only 16 K, probably due to the manipulations used to prepare it, resulting in a local loss of oxygen. The characteristic has the shape of an inverted V, in agreement with the theo-

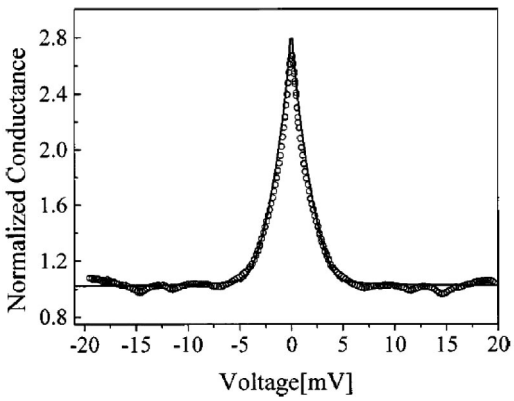

FIG. 12. Measured conductance characteristic of a $Au/La_{2-x}Sr_xCuO_4$ single-crystal underdoped contact. The data were fitted for a nodal direction, giving $Z=0.3$, and a gap of 5 meV. Adapted from Dagan *et al.*, 2000.

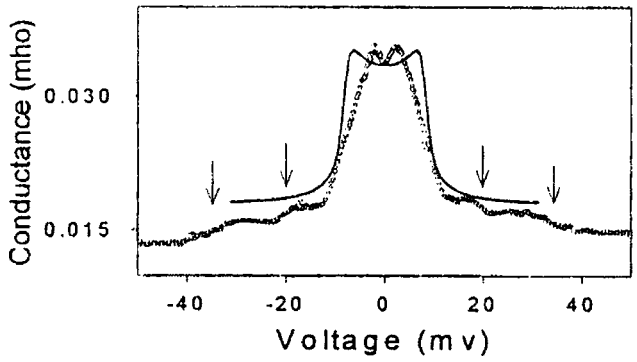

FIG. 13. Measured conductance characteristic of a $Au/La_{2-x}Sr_xCuO_4$ single-crystal contact near optimum doping. Note the small split of the conductance peak at small bias. The line is an attempt to fit the data with an *s*-wave gap. Arrows indicate high-bias structures possibly related to phonons. Adapted from Achsaf *et al.*, 1996.

retical predictions for a low-Z (110) surface (Fig. 7). A fit to theory gives $\Delta=5$ meV. This result will be important when we discuss the underdoped regime (pseudogap regime) in the next section.

Low-Z contacts on LSCO at actual optimum doping have slightly different characteristics. Figure 13 shows that of a contact obtained by electromigration (Achsaf *et al.*, 1996). Upon making contact between the tip and the sample, the resistance was first very high, in the 100-kΩ range, presumably due to an oxygen-depleted surface layer. A positive bias was then applied to the tip, possibly attracting positively charged oxygen ions from the bulk of the sample towards the surface. The general shape of the characteristic is still that of an inverted V, but with a local minimum near zero bias. As explained in the theory section, this local minimum is incompatible with a pure *d*-wave symmetry.

Etching the surface is another way to obtain a low-Z contact. On the same crystal, this method produced characteristics of the same general shape as that obtained on a junction prepared by electromigration, discussed above, but with a wider separation between the two peaks. It may be that etching exposes other crystallographic facets besides (110), giving a characteristic more like that obtained on (100) surfaces. Similar characteristics were obtained by Gonelli and co-workers (Daghero *et al.*, 2002) on polycrystalline LSCO samples. They were also interpreted as indicating a mixed symmetry.

Concerning the gap value, Achsaf *et al.* (1996) conclude from their low-Z data that it is of about 9 meV in a slightly underdoped LSCO single crystal. This is somewhat smaller than the value of the gap obtained from tunneling contacts on the same crystal, which is closer to 15 meV.

Relatively low-Z contacts ($Z=1$) were obtained by Wei *et al.* (1998) on an optimally doped YBCO single crystal by driving a Pt-Ir tip into the sample. The characteristics also had the shape of an inverted V. The gap value extracted from the fit is 27 ± 4 meV. For comparison, a regular scanning tunneling microscope (STM) measurement taken along the *c* axis on the same crystal gives a gap value of 19 ± 4 meV.

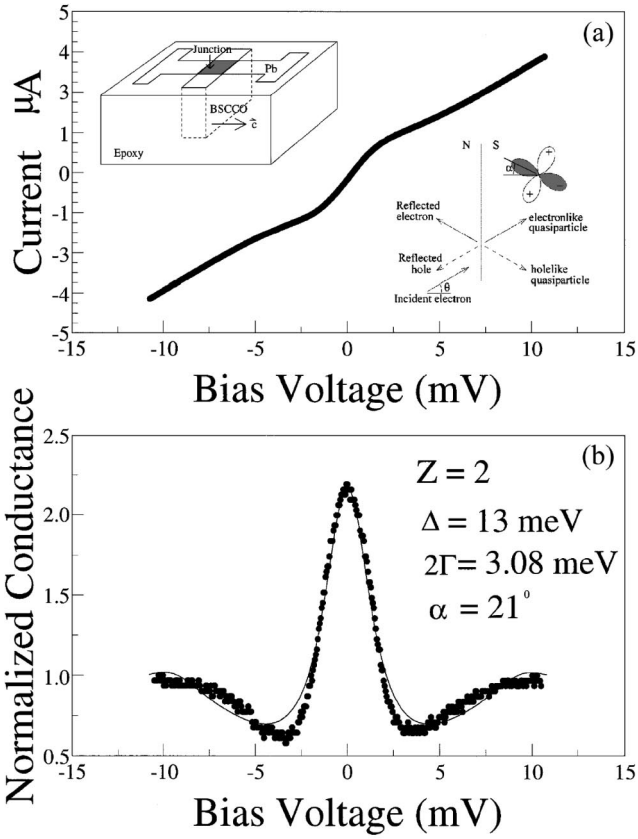

FIG. 14. $I(V)$ and conductance characteristics of an in-plane contact to a $Bi_2Sr_2CaCu_2O_8$ single crystal. Note the return to the normal-state conductance at about 10 meV. Adapted from Sinha and Ng, 1998.

2. High-Z (110) contacts

In agreement with theory, high-Z contacts to (110)-oriented surfaces show a zero-bias conductance peak and a weak structure at the gap edge.

Sinha and Ng (1998) have produced tunnel junctions on the edges of BSCCO single crystals by evaporating onto them a Pb or Ag counterelectrode. The roughness of the edge is large (3000 Å), therefore there is no well-defined surface orientation. Taking this orientation as a free fit parameter, and a smearing factor of 3.08 meV, Sinha and Ng (1998) obtained a good fit of their data to the theory of Kashiwaya *et al.* (1995), with $Z=2$ and $\Delta=13$ meV. One can see from Fig. 14 that the zero-bias conductance is larger than the normal-state conductance by a factor larger than 2, and that the gap edge has a weak signature as a dip below the normal (high-bias) conductance value followed by a progressive recovery. The T_c of the junction was 75 K, presumably indicating underdoping at the surface, either intrinsic or provoked by the contact with the counterelectrode. The rather small gap value will be commented upon in relation to the pseudogap issue in the next section.

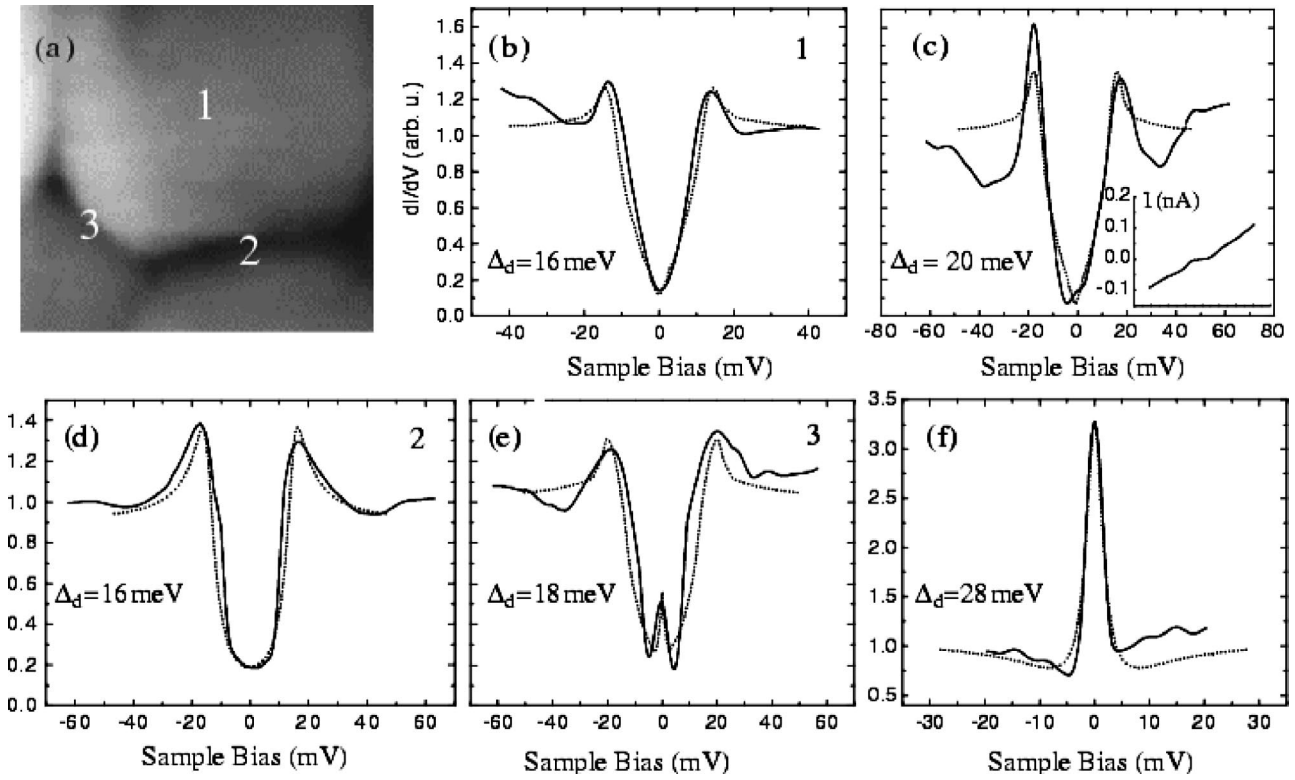

FIG. 15. Measured scanning tunneling microscope (STM) conductances at various positions on an YBCO grain having a (001)-oriented upper surface. The shape of the characteristics goes from V shape on top of the grain (b, c), to U shape near a (100) face (d), to inverted V near a (110) face (e, f). Adapted from Sharoni *et al.*, 2001.

Wei *et al.* (1998) measured the characteristics of STM tunnel junctions on (110) faces of YBCO single crystal. They showed a large zero-bias conductance peak, the conductance at zero bias reaching up to eight times the normal-state value. As predicted by theory, the peak is followed by a dip before return to the normal-state (high-bias) value. The gap value obtained from the fit is 27 ± 4 meV.

In general, the highest zero-bias conductance peaks have been obtained on STM junctions. The scanning tunneling microscope neatly reveals the large anisotropy in the total density of states of the high-T_c superconductor. Sharoni *et al.* (2001) have reported observing, on the same sample, a *c*-axis oriented YBCO film, three types of characteristics: V shaped on (001) areas, zero-bias-dominated on (110) grain edges, and flat bottomed on (100) edges (Fig. 15; see also Sharoni *et al.*, 2003). These observations show that the total density of states can vary over a length scale of the order of a nanometer. On (110)-oriented films, a zero-bias conductance peak and a gaplike feature are both observed (Sharoni *et al.*, 2002). Macroscopic contacts allowing in-plane tunneling into films having the (100) or (110) orientations have been produced by a number of techniques, such as using a Pb counterelectrode (sometimes with a thin Ag buffer layer in order to avoid massive oxygen out-diffusion; see Lesueur *et al.*, 1992) or a copper counterelectrode (Aprili *et al.*, 1999). The method that we have used most of the time is to stick a small In dot on the fresh surface of the film (Krupke and Deutscher, 1999). These contacts are very stable and can sustain repeated thermal cycling without damage. The exact nature of the dielectric layer is not known. It may be the result of some loss of oxygen at the surface, resulting in an underdoped YBCO insulating surface, or it may be due to oxidation of the In counterelectrode by oxygen diffusing out from the YBCO layer. The process appears to be self-limited (this is not the case with a Pb counterelectrode, which "pumps out" oxygen so effectively that the underlying YBCO film can become insulating). Millimeter-size contacts have typical resistances in the convenient range of 10–100 Ω. These junctions do not yield characteristics as ideal as those that can be obtained by STM, apparently due to surface roughness and to the high sensitivity of the total density of states to faceting on the nanometer scale, as demonstrated by the STM observations of Sharoni *et al.* (2001). (110) facets actually act as shorts, but the junctions have a significant advantage in that they allow measurements to be easily taken as a function of temperature and applied magnetic field.

A typical characteristic obtained by this method on a (110)-oriented film is shown in Fig. 16. Compared to STM data, the zero-bias conductance peak is considerably smeared. On the other hand, a gaplike feature is well pronounced. This gaplike-feature peak has been interpreted within the framework of the Kashiwaya *et al.* (1995) theory as resulting from surface roughness (Fogelstrom *et al.*, 1997), which has about the same effect as if the surface had an effective orientation intermediate between (100) and (110). Actually, there is not much dif-

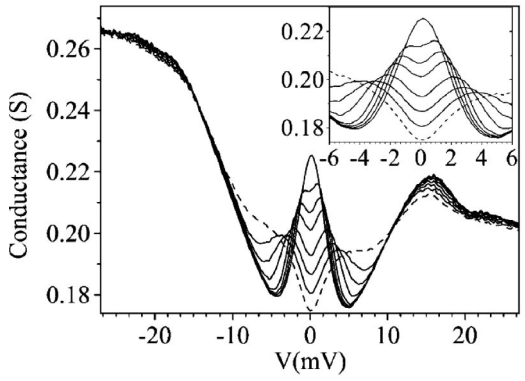

FIG. 16. Tunneling characteristics of an In/YBCO junction on a (110)-oriented film at increasing magnetic fields of up to 6 T. Inset: measurements in decreasing fields. Adapted from Dagan and Deutscher, 2001a.

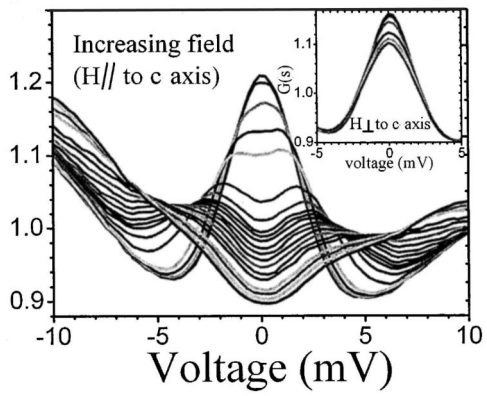

FIG. 17. Tunneling characteristics of an In/YBCO junction in increasing fields. The YBCO film has the (110) orientation, and the field is oriented parallel to the surface of the film and parallel to the *c* axis (itself in-plane oriented). Note (inset) that the splitting does not take place when the field is applied perpendicular to the *c* axis. Adapted from Beck, 2004.

ference between the characteristics of macroscopic junctions prepared on (100)- and (110)-oriented films. They show similar zero-bias conductance peaks and gaplike features. A quantitative fit to the data, taking into account surface roughness, has been presented by Fogelstrom *et al.* (1997). The gaplike feature is well reproduced. Its peak position is somewhat below the value of the gap. Experimentally, its position is extremely reproducible from sample to sample (optimally doped), and from laboratory to laboratory. It is, in fact, one of the most reliable pieces of data to be found in the high-T_c superconductor literature. Its position is 17 mV for optimally doped YBCO, with a variation of less than 1 mV between data originating from different laboratories. Fogelstrom *et al.* (1997) determined that the gap value might be up to 50% higher, or about 25 meV, depending on the exact surface orientation spread. Assigning to the ASJ gap in optimally doped YBCO a range of 20–25 meV is a safe estimate.

3. High-*Z* (110) contacts under magnetic fields

Lesueur *et al.* (1992) were the first to notice that a magnetic field can induce a split of the zero-bias conductance peak in YBCO films, and proposed that it might be due to a Zeeman effect, under the assumption that the conductance peak itself is due to the presence of magnetic impurities in the vicinity of the barrier. Covington *et al.* (1997) further studied this effect, which was given a different interpretation by Fogelstrom *et al.* (1997) in terms of a Doppler shift of the energy of the ASJ surface states. This Doppler shift is due to the superfluid velocity corresponding to the field-induced Meissner currents. The experimental proof that the zero-bias conductance peak is not primarily due to the presence of magnetic impurities was given by Krupke and Deutscher (1999) and by Aprili *et al.* (1999). With films having a good in-plane orientation of the *c* axis, they showed that the zero-bias conductance-peak field splitting is very anisotropic, being strong when the field is oriented perpendicular to the CuO_2 planes and undetectable when it is in the orthogonal direction (Fig. 17). It is in the first geometry that Meissner currents flow along the CuO_2 planes. If the zero-bias conductance peak had been of magnetic origin, its splitting should have been isotropic.

In the model of Fogelstrom *et al.* (1997), the energy of the ASJ states is Doppler shifted by an energy equal to $v_S \cdot p_F \cos\Theta$, where v_S is the superfluid velocity associated with the Meissner currents, p_F is the Fermi momentum, and Θ is the angle that the trajectory of a tunneling quasiparticle makes with the surface of the sample. At low fields, theory predicts that since v_s increases linearly with the applied field, so should the zero-bias conductance-field splitting, as indeed has been observed experimentally (nonlinear effects may arise due to the presence of a *s*-wave channel; Fogelstrom *et al.*, 2003). Saturation is predicted to occur at fields of the order of the thermodynamical critical field H_c as observed by Covington *et al.* (1997; Fig. 18). The strong anisotropy of

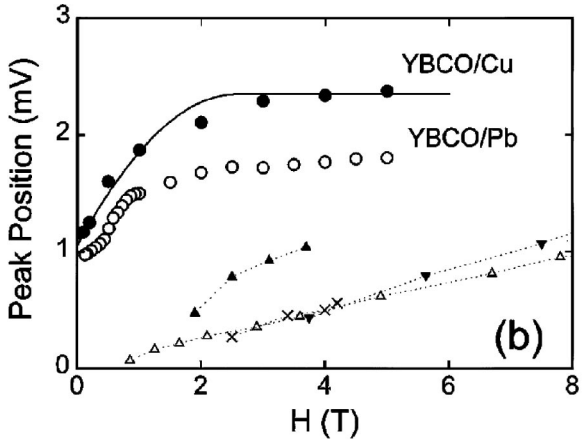

FIG. 18. Field dependence of the zero-bias conductance peak for in-plane junctions to YBCO films. The fit for the YBCO/Cu contact is from the theory of Fogelstrom *et al.* (1997). Adapted from Covington *et al.*, 1997.

the zero-bias conductance-peak field splitting, and its field dependence, strongly support the idea that d-wave symmetry is at the origin of the zero-bias conductance peak. The model of Fogelstrom *et al.* (1997) assumes that vortices do not penetrate into the sample for fields of up to the order of H_c, or, in other words, that there exists a strong Bean-Livingston (Bean and Livingston, 1968) barrier. Since there is no such barrier against vortices' exiting in decreasing fields (Bussières, 1976), a strong hysteresis of the zero-bias conductance-peak field splitting is expected. Again, this is in general agreement with experiment, the splitting being larger in increasing than in decreasing fields (Krupke and Deutscher, 1999). In fact, according to the Doppler-shift model based on the Bean-Livingston currents, there should be no zero-bias conductance-peak splitting at all, or only a small one, in decreasing fields. It is also expected that the splitting should be strongly decreased at thicknesses smaller than the London penetration depth λ, for which Meissner currents reduce as the thickness divided by λ. Both predictions are again in agreement with early results obtained on films that had the (100) orientation (Krupke and Deutscher, 1999) or the (103) orientation (Covington *et al.*, 1997). For such films, the very existence of the zero-bias conductance peak is supposedly due to surface roughness. Later results, obtained on films that did have the (110) orientation, show a more complex behavior. In particular there is a strong splitting in decreasing fields, and it persists even at small thickness (Dagan and Deutscher, 2001b; Beck *et al.*, 2003). This behavior raises questions that will be discussed in the last section of this review.

V. ASJ SPECTROSCOPY AND THE PSEUDOGAP ISSUE

Andreev–Saint-James spectroscopy allows a good determination of the gap in the cuprates, it gives solid evidence that they have well-defined quasiparticles, and it provides a good estimate of their mass renormalization. ASJ spectroscopy is also a phase-sensitive tool. More will be said on this last topic when we discuss the occurrence of minority components of the order parameter in the last section of this review. It turns out that ASJ spectroscopy also sheds light on the possible origins of the pseudogap, one of the least understood features of the cuprates.

A. Manifestations and possible origins of the pseudogap

There exists converging experimental evidence from NMR spin-susceptibility measurements (Alloul *et al.*, 1989), heat-capacity measurements (Tallon and Loram, 2001), ARPES (Ding *et al.*, 1996), optical measurements (see the review by Timusk and Statt, 1999), and tunneling experiments (Racah and Deutscher, 1996; Miyakawa *et al.*, 1997; Renner *et al.*, 1997) that in underdoped cuprates there is a loss of states at the Fermi level below a temperature $T^*(p)$ that increases as the doping p is decreased. T^* and T_c have opposite variations as p is reduced below the optimum level p_M. This loss of states occurs over a certain energy range, called the pseudogap, which can be measured by different spectroscopic methods. There are even today sharply conflicting views on its origin. From a phenomenological standpoint, these views can be grouped into two classes: one holds that the pseudogap is a high-temperature precursor of the superconducting state, the other that it is strictly a normal-state property, with no direct relation to superconductivity. In the first case, T^* is the temperature below which a pairing amplitude appears, without the phase coherence, which is achieved at a lower critical temperature T_c; it follows necessarily that $T^* > T_c$. In the second case, T^*, being a normal-state property, is not necessarily larger than T_c. In the first case, there cannot be a crossing point between $T^*(p)$ and $T_c(p)$; in the second case, there may be one.

Friedel (1988, 1989) has applied the concept, developed by Mott (cited by Friedel, 2004) to describe the effects of coherent diffraction of valence electrons from a local atomic order in liquid or amorphous metals or Hume-Rothery alloys, to the case of local 2D antiferromagnetic order. The term "pseudogap" that he introduced describes a density of states resembling that resulting from long-range antiferromagnetic order, with a gap and peaks at the gap edges, but with states within the gap and broadened peaks.

By contrast, other authors have seen the pseudogap as a high-temperature precursor to superconductivity. An early model is the bipolaronic approach of Alexandrov and Mott (1994). Chen *et al.* (2004) have investigated the regime of BCS-to-Bose-Einstein (BE) crossover with the emphasis on finite-temperature effects. They find that, in the crossover region, the order parameter is distinct from the gap in the single-particle excitation spectrum, going to zero at T_c while the gap remains finite, and going smoothly into the pseudogap regime above T_c. In the ground state, as seen in a low-temperature spectroscopic experiment, there is only one single energy scale, the order parameter and the gap being identical. In yet a different approach, Bernevig *et al.* (2003) have studied the effect of strong Coulomb effects on superconductivity. They find that these effects generate a d-wave gap, and at the same time reduce the superfluid density. The stronger they are, the larger the gap value and the smaller T_c will be because of Kosterlitz-Thouless effects (Emery and Kivelson, 1995). The transition to the insulating antiferromagnetic state occurs at half filling. If Coulomb effects reduce (as may be expected in the overdoped region), there is a smooth transition to a BCS superconductor. In this model, as well as in the BCS-to-BE crossover scheme, the pseudogap is a manifestation of incipient superconductivity.

In a different approach, Perali *et al.* (2000) have studied the consequences of a strong anisotropy, both the effective interaction and the Fermi velocity being momentum dependent. At the antinodes the interaction is strong and the Fermi velocity small, and vice versa at the nodes. One possible mechanism of a strong momentum

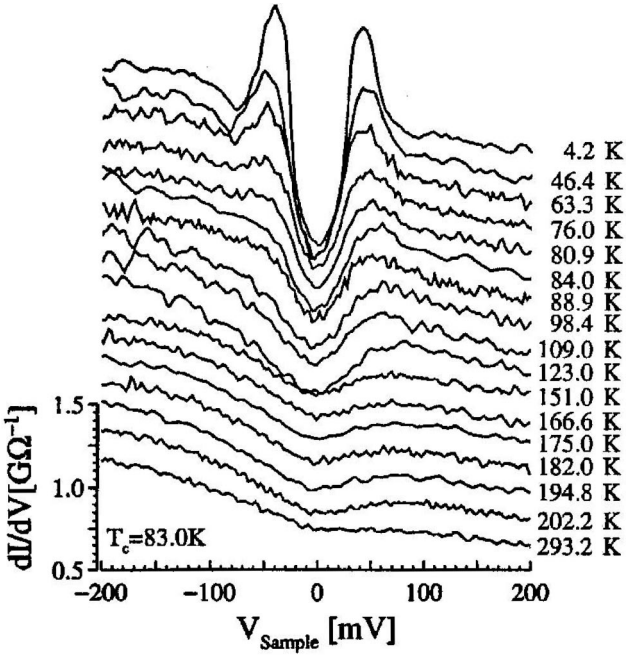

FIG. 19. Scanning tunneling microscope characteristics measured on an underdoped $Bi_2Sr_2CaCu_2O_8$ single crystal, at temperatures ranging from 4.2 K up to room temperature. A conductance dip persists up to the highest temperature. Note, however, the change in the dip amplitude when going from 123 to 151 K. Adapted from Renner *et al.*, 1997.

dependence is a charge instability for stripe formation, occurring below a line $T^*(p)$ that starts from a quantum critical point at $T=0$ near optimum doping. Other theories have emphasized the role of fluctuations around a quantum critical point, causing the appearance of an imaginary component of the order parameter on one side of the quantum critical point (Sachdev, 2000; Ng and Varma, 2004).

Renner *et al.* (1997) performed STM measurements on BSCCO single crystals at different doping levels and observed a pseudogap (with a substantial density of states within it) above T_c, merging into the gap in the superconducting state below T_c. In underdoped crystals, a pseudogap could be observed up to room temperature (Fig. 19). Even in overdoped samples, a pseudogap was seen to persist a few tens of K above T_c. In other words, $T^*(p)$ and $T_c(p)$, as measured by tunneling in BSCCO, do not cross each other. This behavior is compatible with the pseudogap's possibly being a precursor of the superconducting gap, as proposed by the authors. An increase of the gap was also measured by break junctions on underdoped BSCCO by Miyakawa *et al.* (1997).

On the other hand, Tallon and Loram (2001) have concluded from an analysis of heat-capacity data on a number of cuprates that $T^*(p)$ and $T_c(p)$ do cross each other, $T^*(p)$ following a linear behavior that extrapolates at zero temperature to a universal "critical" concentration $p_c=0.18$ holes/Cu. They conclude that T^* is not directly related to superconductivity.

Very recently, Alff *et al.* (2003) reported that in the electron-doped compounds PrCeCuO and LaCeCuO, a pseudogap develops only at low temperatures $T<T^*<T_c$, as can be seen by applying magnetic fields strong enough to destroy superconductivity. They conclude that the pseudogap cannot be a precursor to the superconducting state. The absence of a pseudogap opening above T_c in the electron-doped cuprates was also noted by Kleefisch *et al.* (2001), and its presence below T_c noted by Qazilbash *et al.* (2003).

These results (and many others that we have not cited) do not allow one to draw a general conclusion regarding the origin of the pseudogap. It may be that different kinds of measurements, such as tunneling and heat capacity, "see" different pseudogaps. Additionally, it could also be that the pseudogap has different origins in different cuprates. For a review on the pseudogap, see Timusk and Statt (1999).

B. ASJ spectroscopy in the pseudogap regime

The first important observation is that strong ASJ reflections are observed in the pseudogap regime. This is particularly true for ASJ bound states. Zero-bias conductance peaks have been observed in strongly underdoped YBCO (Dagan *et al.*, 2000) and BSCCO (Sinha and Ng, 1998). They persist up to T_c, where they vanish. The second observation is that in the pseudogap regime gap values determined by ASJ spectroscopy and single-particle spectroscopies (tunneling or ARPES) are different, while they roughly agree in the overdoped regime (Deutscher, 1999).

In underdoped YBCO, Yagil *et al.* (1995) reported measurements of ASJ reflections by point contact on *a*-axis films [(100)-oriented surface] yielding a gap value of 13 meV. The enhancement of the conductance below the gap was weaker than in optimally doped YBCO. Giaever tunneling on similarly underdoped *a*-axis films, with T_c values in the range of 40–60 K, gives a gap of 40–50 meV (Racah and Deutscher, 1996; Fig. 20).

As mentioned above, in an underdoped BSCCO junction close to the (110) orientation and having a $T_c=70$ K, Sinha and Ng (1998) obtained from their fit to the data an ASJ gap of 13 meV. This is much smaller than the 50-meV STM gap value at similar doping (Renner *et al.*, 1997). Aubin *et al.* (2002) prepared tunnel junctions on optimally doped single-crystal BSCCO having a surface passivated by a thin CaF_2 layer. Crystals were cut and polished so as to expose (100)- and (110)-oriented surfaces. On (100) surfaces, broad Giaever-like tunneling curves were obtained with maxima at 37 meV, which is in agreement with STM data (Renner *et al.*, 1997). On (110) surfaces the conductance characteristic had the shape typical of high-Z junctions for that orientation, with a high zero-bias conductance peak followed by a dip before recovery to the normal-state conductance. Recovery occurred in the range of 20–30 meV [Fig. 4(a) and Fig. 2 of Aubin *et al.*, 2002], which we would expect corresponds to the range of possible gap

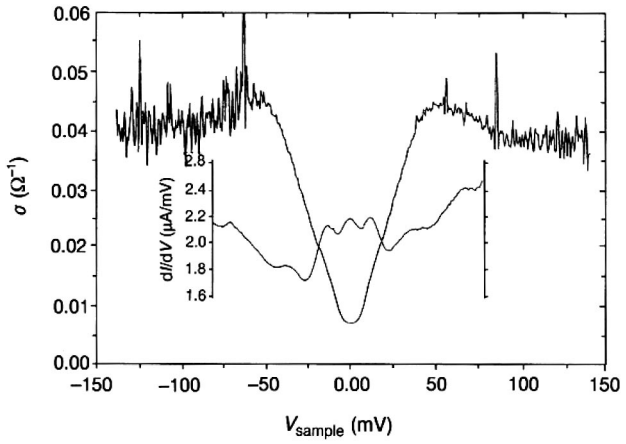

FIG. 20. Comparison between an ASJ (inside graph) and a Giaever characteristic measured on similarly underdoped YBCO samples. Note the difference in energy scales: about 15 meV for the ASJ reflection edge, and 50 meV for the Giaever gap. Adapted from Deutscher, 1999.

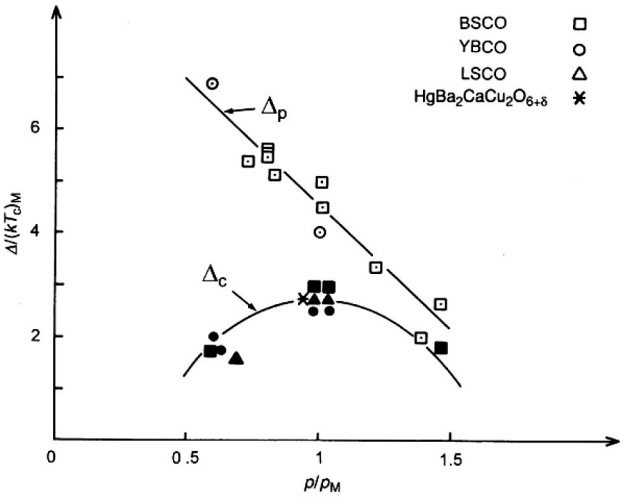

FIG. 21. Behavior of ASJ and Giaever (or ARPES) energy scales as a function of doping in different cuprates. The ASJ scale (Δ_c) follows the same behavior as does T_c while the Giaever scale (Δ_p) keeps rising as the doping is reduced. Adapted from Deutscher, 1999.

values. A fit to these (110) data, considered as reasonable by the authors, was nevertheless given with a gap value of 37 meV. D'Gorno and Kohen (1998) obtained point-contact junctions on a nearly optimally doped (maybe slightly overdoped) BSCCO single crystal that could be fitted very well to a (100) orientation with a gap value of 20 meV and $Z=0.8$ (Fig. 9). We would conclude that, for BSCCO, ASJ spectroscopy [low-Z (100) contacts, moderate, and high-Z (110) contacts, both sets of data being dominated by ASJ reflections] gives for BSCCO a gap of 20–30 meV at or near optimum doping, and less than 15 meV in underdoped samples. By contrast, Giaever tunneling gives gap values of 30–40 meV at optimum doping and 40–50 meV in underdoped samples. Recently, a detailed STM study on BSCCO cleaved crystals, systematically scanning large areas of the crystal, have shown that up to energies in the range of 20 meV, the single-particle tunneling spectra are quite homogeneous across the sample's surface even in underdoped samples (McElroy *et al.*, 2004). By contrast, gap values, as determined by the bias at which the conductance is at a maximum, are quite inhomogeneous and range from 20 meV up to 70 meV. Spectra showing the larger gaps have weak coherence peaks. They correspond to antinodal states, which are quite inhomogeneous in space. These observations are consistent with our report of strong ASJ reflections ranging in energies up to about 20 meV (Deutscher, 1999). This appears to be the energy scale of the superconducting condensate. It does not increase in the underdoped regime.

On LSCO Daghero *et al.* (2002) reported measurements of ASJ gaps that decrease in the underdoped regime, as also seen by Dagan and Deutscher (2001a). As in YBCO and BSCCO, Giaever gaps do increase in underdoped samples.

The following experimental picture then emerges. Strong ASJ reflections occur in optimally doped and overdoped samples for all surface orientations. In underdoped samples, ASJ reflections are weakened on (100) surfaces, but remain strong on (110) surfaces. Gap values obtained from conductance characteristics dominated by ASJ reflections are equal to or smaller than gap values obtained from single-particle tunneling. They decrease in the underdoped regime, following at least qualitatively the doping dependence of T_c (Fig. 21).

At low temperatures, there exists in most cuprates a tunneling pseudogap that increases as doping is reduced. The pseudogap appears in the normal state below a temperature T^*, which can be higher or lower than T_c. In some cuprates, such as BSCCO, $T^* > T_c$ in most (if not all) of the doping range. In other cuprates, the curves $T^*(p)$ and $T_c(p)$ cut each other at some doping level p^*. This is the case for YBCO and even more clearly for the electron-doped compounds. For $p < p^*$, the pseudogap appears above T_c and is larger than the ASJ gap. For $p > p^*$, the ASJ gap and the Giaever gap converge. In that regime the pseudogap does not appear above T_c, but in electron-doped cuprates it may be seen below T_c by applying a field strong enough to quench superconductivity.

C. Compatibility of ASJ reflections and pseudogap models

1. Resonating valence bond and other models emphasizing strong correlation effects

A pseudogap is already implicit in the resonating valence-bond (RVB) model of Anderson (1987), which postulates that electron correlations are the key ingredient in the superconductivity of the cuprates. There may be, however, one major difficulty with this model regarding ASJ reflections, which concerns the nature of electronic excitations. In the RVB model, these are not the usual quasiparticle excitations we are familiar with in

metals, but rather excitations that do not carry at the same time charge and spin (holons and spinons). There is no electron-hole symmetry, and it is not clear whether under these circumstances one could even have strong ASJ reflections, whose very existence implies electron-hole mixing: in a Saint-James cycle, an excitation is electronlike half of the time, and holelike the other half.

This difficulty may be overcome in other models where strong electron correlations play a key role. They include fermion-boson models with electron pockets developing near the nodes as doping is increased (Altman and Auerbach, 2002; for earlier fermion-boson models, see Friedberg and Lee, 1989; Ranninger *et al.*, 1995). In the condensed state, there is a bosonic field that generates a superconducting gap *à la* BCS in the electron pockets, and excitations from this gap would have the usual electron-hole symmetry.

In another recent model originally proposed by Laughlin (Laughlin, 2002; Bernegiv *et al.*, 2003), strong electron correlations come on top of a conventional BCS Hamiltonian. In contrast with the resonating valence-bond model, the nature of electronic excitations is then identical to that in ordinary metals; there are thus no problems with ASJ reflections. Strong correlations continuously increase the value of the BCS gap, while at the same time the superfluid density is reduced, eventually leading to the destruction of superconductivity as a macroscopic coherent phenomenon (Emery and Kivelson, 1995). The (pseudo)gap appearing at high temperatures is then a precursor of superconductivity, before it is quenched altogether. As we shall see below, there are problems with this part of the model.

2. The semiconductor-superconductor and strong-coupling models

Pistolesi and Nozières (2000) have calculated the conductance of N/S contacts within two models compatible with the existence of a gap in the density of states above T_c: one where it is a normal-state property, that is, there is a semiconducting gap Δ_0 due to a competing order such as a charge-density wave (CDW), which has no direct relation to superconductivity (Nozières and Pistolesi, 1999); and another one, in which the pseudogap is a manifestation of a crossover to strong coupling (Bose-Einstein limit) where the energy necessary to break a pair can be much larger than $k_B T_c$ (Leggett, 1980; Nozières and Schmitt-Rink, 1985).

In the normal-state pseudogap scenario, ASJ reflections are reduced by the competing order, which prevents the full conversion of incoming quasiparticles into superfluid. In the strong-coupling limit, ASJ reflections are reduced because of a mismatch of the Fermi wave vectors when the gap approaches the Fermi level. In both cases, there exists an energy gap E_g which is a combination of the normal-state gap, or energy necessary to break a preformed pair, and the superconducting order parameter. In both models, the Blonder-Tinkham-Klapwijk–reflection coefficient $A(\varepsilon)$ is reduced below E_g; this reduction becoming substantial if E_g is large compared to the order parameter Δ. No strong ASJ reflections can then occur.

In the specific example of the semiconductor-superconductor model, the CDW order (Δ_0) induces Bragg reflections and the superconducting order (Δ_m) ASJ reflections. The strongest order determines the penetration depth of the evanescent wave. If Δ_0 is larger, the specular Bragg reflection will build up before the ASJ reflection does. The latter will therefore be weak. A similar conclusion is reached in the strong-coupling limit. In the calculated conductance characteristic, there is no structure at the bias equal to the superconducting order parameter if $\Delta_0 > \Delta_m$, or in the strong-coupling limit.

These results are of a generic nature. They apply to different models of the pseudogap such as the BCS-to-BE crossover (Chen *et al.*, 2004) or models emphasizing strong correlations (Bernegiv *et al.*, 2003) or models of competing orders (Castellani *et al.*, 1997). A subgap structure can be restored if a buffer layer of sufficient thickness is assumed to exist between N and S (Alexandrov and Andreev, 2001), but the origin of such a layer is not clear. They are not in agreement with the experimental findings of strong ASJ reflections, and of an ASJ energy scale smaller than the Giaever gap, in the pseudogap regime, if one assumes that the competing order parameter (or the strong-coupling effects) dominates all around the Fermi surface over the superconducting order parameter.

Note, however, that the calculation assumes that the normal-state gap is a full gap, i.e., that in the normal state there are no states below it. This is, of course, an oversimplification of the experimental situation. For PCCO, in which the normal-state total density of states has been measured at low temperatures (Alff *et al.*, 2003), the zero-bias conductance is still about 80% or more of its normal-state value, so there are, in fact, many states below the pseudogap. Such a high density of states in the pseudogap region is obtained in the model of Friedel and Kohmoto (2002). If these states are conducting, one might expect structures in the conductance characteristic at both biases—the superconducting order parameter and the pseudogap scales. Two energy scales—one where the conductance goes down, marking the ASJ gap, and one where it goes up, marking the pseudogap—are indeed visible in the data of Yagil *et al.* (1995), but no conductance calculations are available for the Friedel-Kohmoto (Friedel and Kohmoto, 2002) pseudogap model that we could compare quantitatively to experiments.

An alternative approach has been tried by Pistolesi (1998), who has shown that a critical current effect may, in fact, introduce into the conductance characteristic a structure at a bias value, typically the phase stiffness Λ, which limits T_c in the strong-coupling or weak-superfluid density limit. As shown, for instance, by Emery and Kivelson (1995), when the superfluid density is very small, T_c is determined by

$$kT_c = (16\pi^3)^{-1}(\Phi_0)^2(a/\lambda^2), \tag{5.1}$$

where Φ_0 is the flux quantum, λ the in-plane London penetration depth, and a a length scale equal to the coherence length in the direction perpendicular to the CuO planes or to the interplane distance, whichever is larger. Pistolesi finds that a critical current effect will reduce the conductance at a voltage V_c given by

$$eV_c = \Lambda(k_F\xi_{\text{phase}})^{-1} \tag{5.2}$$

where the phase ξ_{phase} was calculated by Pistolesi and Strinati (1996) and by Marini *et al.* (1998). In the vicinity of the BCS-to-BE crossover, $k_F\xi_{\text{phase}} \approx 1$, and $eVc \approx \Lambda \approx kT_c$, in agreement with experimental results (Deutscher, 1999).

3. Two-gap model

The Rome group (Perali *et al.*, 2000) has extended the semiconductor-superconductor model of Pistolesi and Nozières (2000) to the case of a *d*-wave order parameter. In this model, the competing order parameter dominates over the superconducting one only in the antinode regions. Specifically, the origin of the pseudogap lies in the vicinity of a charge-density-wave (CDW; Benfatto *et al.*, 2000) line $T^*(p)$, as mentioned above, but from a phenomenological standpoint their main results are given in terms of a gap $\Delta(\phi)$ which is dominated by the pseudogap Δ_p near the antinodal points and by the superconducting order parameter near the nodes. They argue in favor of the weak-coupling limit $\Delta < t$, where t is the nearest-neighbor interaction term in the tight-binding approximation, so that T_c is equal within a numerical factor to the energy scale that governs the behavior of Δ near the nodes. In the overdoped regime, $\Delta(\phi)$ follows the *d*-wave law $\Delta(\phi) = \Delta(0)\cos 2\phi$ over the entire angular range. In the underdoped regime, the value of the gap at the nodal points is uncorrelated with the (larger) characteristic energy scale near the nodes.

This model is qualitatively in agreement with the results of ASJ spectroscopy on (110) surfaces in the underdoped regime as described above. The pseudogap near the antinodal points is larger than the value that the superconducting order parameter would have in the absence of this pseudogap (in the language of Nozières and Pistolesi, $\Delta_0 > \Delta_m$ near the antinodal points). Thus these regions do not contribute to the ASJ reflection amplitude because, for the corresponding **k** vectors, normal quasiparticle reflection occurs before conversion to the condensate takes place. Hence the only energy scale that will appear in ASJ spectroscopy will be that which characterizes the angular dependence of the gap near the nodes, which is the superconducting order parameter, itself proportional to T_c. The fact that for all cuprates studied so far the ASJ spectroscopy energy scale varies with doping as T_c does just means that these cuprates are basically in the weak-coupling limit, as assumed by the Rome group.

More generally, a momemtum dependence of the interactions leading to the pseudogap, whatever its origin may be, seems to be a necessity if agreement with ASJ experiments is to be achieved. This is because these experiments tell us that there is no pseudogap around the nodes. Theories that do not include a momentum dependence, such as those of Chen *et al.* (2004), or Bernevig *et al.* (2003), for which the pseudogap is a *d*-wave gap that becomes the superconducting gap at low temperatures, do not seem to be compatible with the observation of strong ASJ reflections in the underdoped regime.

4. Some comments on the pseudogap

In a previous publication (Deutscher, 1999) I left open the question of the origin of the pseudogap: whether the loss of states at the Fermi level that starts below T^* is due to an emerging pairing amplitude (a strong-coupling effect), or whether it bears no direct relation to superconductivity. Theoretical progress in the analysis of experimental results known at this time and new experiments reviewed in this section, and particularly conclusions drawn from the observation of strong ASJ reflections in the pseudogap regime, present, in fact, serious difficulties for both kinds of models, at least if no momentum dependence is included. Yet I believe that the balance now tilts somewhat against the preformed pairs scenario.

The formation of true bound pairs above T_c, in the sense of a negative chemical potential with respect to the bottom of the conduction band, requires a binding energy of the order of a fraction of the bandwidth, say, of the order of the eV. Pseudogap values determined by ARPES and tunneling reach at most 10% of this value, so there cannot really be bound pairs. More specifically, for $(\Delta/EF) \approx 0.1$, as seen experimentally, strong-coupling theory (Pistolesi and Strinati, 1996) tells us that the two length scales ξ_{pair} (the size of a pair) and ξ_{phase} (the size of a vortex core) differ only by a few percent, and so should the corresponding energy scales. Instead, for moderately underdoped samples (T_c about half of its maximum value), the pseudogap and the ASJ gap differ by a factor of about 4. According to this analysis, the pseudogap is not a strong-coupling effect. Additionally, there should be at low temperatures only one energy scale in the superconducting state (Chen *et al.*, 2004). In the underdoped regime, this is not the case, since the Giaever and the ASJ gaps have opposite doping dependences (Fig. 21). The recent experiments of McElroy *et al.* (2004) also establish that there is no correlation between homogeneous, low-energy excitations in the nodal regions and large gaps in the antinode regions.

Ruling out the pseudogap as a homogeneous precursor of superconductivity in real space and in momentum space does not mean that the cuprates are strictly in the BCS weak-coupling limit. In fact, they are not far from the BCS-to-BE crossover, defined as shown by Pistolesi and Strinati by the condition $(k_F\xi_{\text{pair}}) = 1$. One of the manifestations of this proximity is the Uemura plot $T_c \propto \lambda^{-2}$ followed by all underdoped cuprates (Uemura, 2002). Another is the observation of strong fluctuation effects in the heat-capacity transition. These measure-

ments allow us, in fact, to draw a fine distinction between different cuprates in terms of their proximity to the BCS-BE crossover. The heat-capacity transition in YBCO can be analyzed in terms of a mean-field jump with additional fluctuation effects (Marcenat *et al.*, 1996; Junod *et al.*, 1999). These fluctuation effects become quite weak in overdoped samples (Junod *et al.*, 1999), for which the transition becomes more and more BCS-like as doping is increased. In contrast, no mean-field jump can be identified in BSCCO, for which fluctuation effects clearly extend several tens of K above T_c, consistent with its being closer to the BCS-BE crossover than is YBCO. Enhanced fluctuations may also reflect the more 2D nature of BSCCO. But a closer proximity of BSCCO to the BCS-BE crossover is also consistent with spectroscopy results. At optimum doping, the Giaever gap in BSCCO (about 30–40 meV) is larger than that in YBCO (about 20 meV). Also, the coherence length as measured by the radius of the vortex core is shorter in BSCCO than it is in YBCO (Fischer *et al.*, 1998). These are clear indications that, at comparable doping levels, BSCCO is closer than is YBCO to the condition $(k_F\xi_{\text{pair}})=1$.

The STM pseudogap data of Renner *et al.* (1997; Fig. 19) on underdoped BSCCO reveal that there may be a difference between characteristics measured up to 121 K, and above that temperature. The former indeed bear a strong resemblance to those measured immediately below T_c, while the latter show only a weak anomaly that remains essentially temperature independent up to room temperature. This suggests that there might be both a superconductivity-related pseudogap between T_c and 120–130 K, and a normal-state pseudogap at higher temperatures. More data are needed here to clarify the situation.

As for YBCO, the quasi-mean-field behavior of the heat capacity at optimum doping is fully consistent with the absence of a pseudogap in tunneling, as well as with the fact that the Giaever and ASJ gaps are identical. YBCO is, in fact, the only cuprate that clearly breaks away from the Uemura plot. By overdoping it with oxygen up to O_7, one can increase its superfluid density up to a factor of 2 over its value at optimum doping, while T_c remains almost constant (it only goes down by a few degrees; Bernhardt *et al.*, 1995). In the overdoped regime, YBCO presents all the characteristics of a strict BCS superconductor: a critical temperature independent of the superfluid density, a sharp heat-capacity transition, and an identity between the Giaever and ASJ gaps. It would be really surprising if nearly optimally doped BSCCO, not so different after all, would show precursor effects of superconductivity at temperatures up to room temperature. Maybe such strong precursor effects could be found in more strongly underdoped cuprates if the condition $(k_F\xi_{\text{pair}})$ could be reached. Research is still going on in this area.

VI. SYMMETRY STUDIES AND SPIN EFFECTS

In this last section, I would like to mention two topics of current interest in ASJ spectroscopy: effects on the symmetry of the order parameter in the cuprates of different perturbations such as nonoptimum doping, applied magnetic fields, and proximity with a normal metal. A few words on spin effects are added at the end of this section.

Phase-sensitive experiments are the only ones that can lead to definite conclusions regarding the symmetry of the order parameter. Such were the cornerstone experiments of Wollman *et al.* (1993) on superconducting quantum interference devices (SQUID's) and those of Tsuei and Kirtley (2000a, 2000b) that established that the order parameter in the cuprates has a dominant *d*-wave symmetry. These experiments have, however, left two interesting issues unresolved. First, because they measure phase differences of the order parameter at surfaces or interfaces (grain boundaries), they are not sensitive to possible changes of the symmetry between the surface and the bulk. Muller has recently raised this issue and has argued that an *s*-wave channel may, in fact, dominate in the bulk (Muller, 2004). Second, they are not well suited to detecting the existence of a small imaginary minority component. In the experiments of Tsuei *et al.*, for instance, the signature of pure *d*-wave symmetry is a spontaneous half flux quantum at a tricrystal junction. A small id_{xy} component would only slightly modify this flux value and would be undetected if this change were smaller than the margin of error in the measured value. Additionally, these experiments were plainly not designed to study possible effects of strong applied fields on the symmetry of the order parameter. ASJ spectroscopy is ideally suited to answer such questions. ASJ bound states are very sensitive to the existence of a small imaginary component of the order parameter, which has the immediate effect of removing the nodes. Finally, ASJ spectroscopy can be easily performed under applied fields.

The formalism of Kashiwaya *et al.* (1995) can be used to calculate $I(V)$ characteristics for any order parameter $\Delta(\phi)$. For instance, for

$$\Delta(\phi) = \Delta_0 \cos 2\phi + i\Delta_1 \sin 2\phi \tag{6.1}$$

(the $d+id$ symmetry), the (110) zero-bias conductance peak is split (peak to peak) by Δ_1. The same holds for a $(d+is)$ symmetry. Such symmetries have been discussed by Yang and Hu (1994) and Hu (1994). These order parameters break time-reversal symmetry, implying the flow of boundary currents (Laughlin, 1998).

A. ASJ bound states under applied fields

Meissner screening currents also lead to a split of the zero-bias conductance peak, as discussed in Sec. IV. When a zero-bias conductance peak splits under an applied field, how can we know whether it does so because of field-induced Meissner currents or because it is the field itself (not the currents) that has induced a change in the symmetry of the order parameter, as proposed, for instance, by Laughlin (1998)?

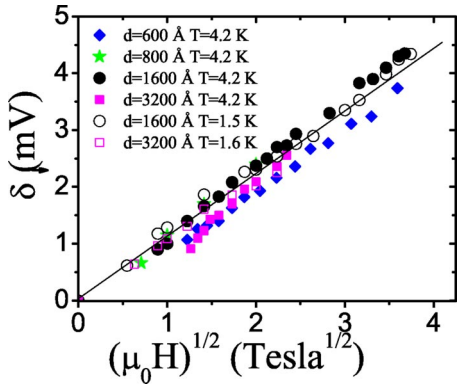

FIG. 22. (Color in online edition) Split of the zero-bias conductance peak in a number of In/YBCO junctions on (110)-oriented films of different thickness, measured in decreasing fields. The split follows a square-root law, with a coefficient of the order of 1 $mV/T^{1/2}$. Adapted from Beck *et al.*, 2004.

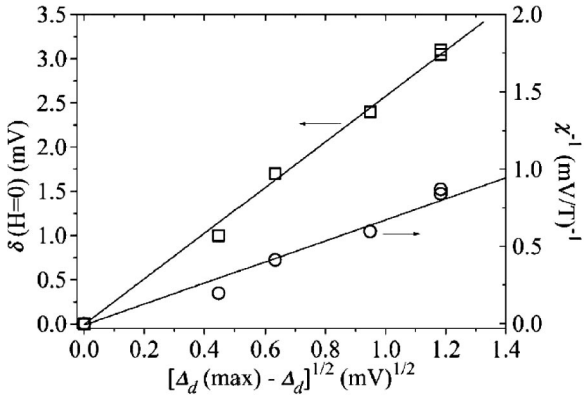

FIG. 23. Dependence of the spontaneous zero-bias conductance-peak split in In/YBCO junctions on (110)-oriented films, as a function of a parameter proportional to the doping level. Overdoping was achieved by increasing the oxygen content. A spontaneous split is only found in overdoped samples. The inverse of the initial slope of the zero-bias conductance-peak field splitting, or susceptibility, is also shown. The susceptibility diverges near optimum doping. The behavior of the spontaneous splitting and of the susceptibility is indicative of the presence of a quantum critical point near optimum doping, beyond which the order parameter develops a small imaginary component. Adapted from Dagan and Deutscher, 2001.

Beck *et al.* (2004) remarked that the current effect should cancel out in decreasing fields, because it is known that there is no Bean-Livingston surface barrier against flux exit. A zero-bias conductance-peak split in decreasing fields, if observed, should therefore be primarily a field effect, and not a current effect. Beck *et al.* measured such a split in the characteristics of junctions prepared on (110)-oriented YBCO films, and showed that it follows the law

$$\delta(B) = AB^{1/2}, \tag{6.2}$$

where 2δ is the conductance-peak split expressed in meV, $A = 1.1$ $meV/T^{1/2}$, and B is the field in tesla. This law was found to hold up to a field of 16 T (Fig. 22). It is in agreement with a prediction by Laughlin (1998) regarding the amplitude Δ_1 of a field-induced id_{xy} component. Node removal costs an energy proportional to $|\Delta_1|^3$, but an energy proportional to $(B \cdot \Delta_1)$ is gained because of the magnetic interaction with the field of the moment produced by the circulating currents proportional to the amplitude of the id_{xy} component. Minimization of the sum of the two terms leads to a law of the form (6.2). The value of the coefficient A found experimentally is in quantitative agreement with theory.

B. Doping effect on the symmetry

Covington *et al.* (1997) reported a spontaneous split of the zero-bias conductance peak in YBCO in-plane tunneling, and interpreted it as an effect of spontaneous time-reversal symmetry breaking. Fogelstrom *et al.* (1997) proposed that this spontaneous split results from the emergence at the surface of an *is* component of the order parameter, an emergence made possible by the local depression of the main *d* component.

Dagan and Deutscher (2001a) reported that in YBCO the spontaneous zero-bias conductance-peak split occurs only in overdoped samples, where it follows the law

$$\delta = C(p - p_M), \tag{6.3}$$

where p is the doping level and p_M its optimum value (at maximum T_c; see Fig. 23). These results were obtained on oxygen-overdoped films. A similar law was reported by Sharoni *et al.* (2002) on Ca-overdoped YBCO films.

There is no direct way to know from tunneling measurements whether the spontaneous imaginary component supposedly responsible for the zero-bias conductance-peak split has *s* or d_{xy} symmetry. An *s* symmetry would mean that the strength of the subdominant *s* channel, emerging at the surface as postulated by Fogelstrom *et al.* (2003), has a strong doping dependence. Alternatively, the imaginary component might be a bulk property. Friedel and Kohmoto (2002) predicted that an id_{xy} component should appear in the overdoped regime, while the symmetry is pure *d*-wave in the underdoped one, as reported by Dagan and Deutscher (2001a). In their theory, the *d*-wave symmetry does not come about because of the interaction responsible for pairing, but rather due to the symmetry of the carrier wave function. Yet another possibility is that the change of symmetry at optimum doping reflects the existence of a quantum critical point (Sachdev, 2000; Dagan and Deutscher, 2001a).

Some ASJ data indicating a possible change of symmetry near optimum doping are also available on LSCO (Achsaf *et al.*, 1996; Dagan *et al.*, 2000) and on the electron-doped PCCO (Qazilbash *et al.*, 2003). The electron-doped cuprates had long been considered an exception to *d*-wave symmetry (Fournier *et al.*, 1998), *inter alia* because of the absence of a zero-bias conductance peak (Alff *et al.*, 1997). More recent tricrystal ex-

periments (Tsuei and Kirtley, 2000a, 2000b) indicated a *d*-wave symmetry. But very recently, a change of behavior of PCCO has been reported as a function of doping, including the ASJ data of Qazilbash *et al.* (2003) already mentioned, and penetration-depth data in overdoped PCCO is better fitted by a nodeless order parameter (Skinta *et al.*, 2002). It could well be that the long-standing controversy on the symmetry of the order parameter in the electron-doped cuprates is on its way towards a resolution in terms of a doping dependence. Electron-doped cuprates are naturally overdoped, which may explain the early results pointing to a nodeless behavior.

A doping-dependent symmetry, if confirmed as a bulk property, would be of some consequence for our understanding of the mechanism for high-T_c superconductivity. Many of the proposed theoretical models, such as the (t,J) models, give a prominent role to the antiferromagnetic coupling parameter J, with this interaction being the primary coupling channel. A pure *d*-wave symmetry necessarily follows in such models, at any doping level. In contrast, in the model of Friedel and Kohmoto (2002), the *d*-wave symmetry does not follow from the pairing interaction itself, but rather from the symmetry of the electronic wave functions, as they are affected by the proximity of the antiferromagnetic state. In that case, Friedel and Kohmoto show that the order-parameter symmetry changes with doping, and in a manner that fits the experimental observations of Dagan and Deutscher (2001a), an imaginary component appearing beyond optimum doping. In fact, it has been claimed very recently on the basis of high-temperature expansions in the thermodynamical limit that the one-band (t,J) model does not lead to a superconducting state (Pryadko *et al.*, 2004), contrary to what had been proposed earlier from numerical work on finite-size systems. So it may be that more conventional interactions such as the electron-phonon interaction will now receive renewed attention.

C. Proximity effect on the symmetry

Wei *et al.* (1998) noted the possibility of a proximity effect between a normal tip and YBCO resulting in a partial *s*-wave character of the order parameter in the latter. Daghero *et al.* (2002) studied low-Z contacts ($Z<0.5$) on LSCO samples as a function of Sr doping. They analyzed the conductance characteristics in terms of a complex order parameter and determined the intensity of each component as a function of doping. They found them to be of the same order. This is in sharp contrast with results obtained on high-Z contacts with YBCO, described in the preceding subsection. There, the *is* (or *id*) component is never more than a fraction of the dominant *d* component. Kohen *et al.* (2003) recently reported a systematic study of the intensity of the minority component in YBCO as a function of the barrier transparency, for point contacts having all $Z<1$ (Fig. 24). They conclude that the value of Z has a strong influence on the intensity of this component, which, according to their analysis, has the *is* symmetry. At low-Z values, both components have similar values. The *is* component diminishes quickly for $Z>0.5$. The authors interpret their results in terms of a proximity effect. They argue that a good contact with the normal metal depresses the *d*-wave order parameter near the interface, because this symmetry channel is very unfavorable for a proximity-induced order parameter in N. In the presence of a subdominant *s*-symmetry channel in S, that symmetry can then manifest itself near the interface. An interesting observation by Kohen *et al.* (2003) is that the excitation gap for the case of a $(d+is)$ order parameter, $\Delta_g=(\Delta_d^2+\Delta_s^2)^{1/2}$, does scale with T_c, meaning that it retains at the surface its bulk value, although the respective weights of the two components vary with Z from junction to junction.

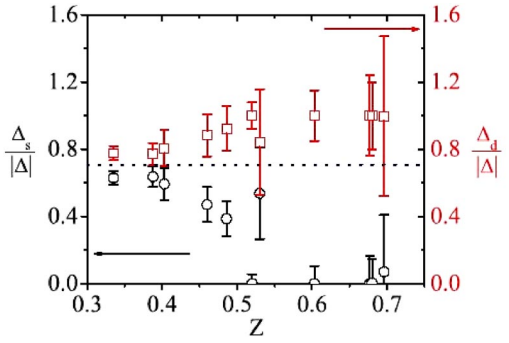

FIG. 24. (Color in online edition) Variation with the barrier parameter Z of the *d*-wave component and of the *is*-wave component at Au/YBCO contacts fitted to the (100) orientation. The *is* component becomes of the order of the *d*-wave one for high-transparency barriers, suggesting that it is due to a proximity effect. Adapted from Kohen *et al.*, 2003.

D. Spin effects

ASJ reflections are profoundly modified at the interface with a ferromagnetic metal. This topic was recently reviewed by Zutic *et al.* (2004). As the spin polarization increases, the conductance of a Sharvin contact at subgap voltages decreases: spin conservation requires that the ASJ reflected hole have a spin opposite to that of the incoming electron, a process incompatible with full spin polarization in the ferromagnet (de Jong and Beenakker, 1995). This has been verified experimentally (Soulen *et al.*, 1998; Upadhyay *et al.*, 1998). Zutic and Valls (1999, 2000) have, however, pointed out that this low-bias conductance decrease as the polarization is increased is only a general property for contacts in which the Fermi velocities of both sides are nearly matched. When they are not, the zero-bias conductance may in fact initially rise with the polarization. Care should therefore be exercised when one attempts to extract the value of the polarization from conductance curves. Using for the fit the Blonder-Tinkham-Klapwijk parameter Z, which does not distinguish between the effect of a dielectric barrier and that of a Fermi velocity mismatch, may not be jus-

tified. Chen *et al.* (2001) have studied transport across the interface between an YBCO layer and a high-spin-polarized oxide. They conclude that spin polarization tends to diminish the zero-bias conductance-peak feature. There has recently been experimental interest in spin injection from ferromagnets into high-T_c cuprates (Dong *et al.*, 1997; Vas'ko *et al.*, 1997; Fu *et al.*, 2002). Ngai (2004) has developed an injection scheme allowing a simultaneous STM measurement and has shown that spin injection reduces and broadens the zero-bias conductance-peak feature. Theoretical treatment has taken into account the influence of ASJ reflections at the interface, including the effect of *d*-wave symmetry, and particularly that of surface bound states (Kashiwaya *et al.*, 1999; Merril and Si, 1999; Zhu *et al.*, 1999; Zutic and Valls, 1999).

Mesoscopic studies of ASJ reflections cover a large field that could be the subject of a review all by itself. We limit ourselves here to a particular situation that is drawing increasing attention, that in which two ferromagnetic tips in close proximity are in contact with a superconductor, the distance between them being shorter than the coherence length. If we assume that the tips are fully polarized, that they are connected to a busbar, and that a difference of potential is applied between this busbar and the superconductor, then an electron coming from one of the ferromagnetic legs cannot be ASJ reflected as a hole in that same leg. It can, however, be reflected in the other leg, provided the polarizations in the two legs are antiparallel (Deutscher and Feinberg, 2000). As a result, the resistance of the device will depend on the relative magnetic polarizations of the two legs: it will be high if they are parallel, low if they are antiparallel. One can consider the device as a kind of transistor—the resistance can be modified by applying a local magnetic field that can reverse the polarization of one of the two legs. More fundamentally, in the case of antiparallel polarizations, the incoming electron in one leg and the reflected hole in the other can be considered as two electrons of the same Cooper pair separated in space, a situation that can have interesting implications (Recher and Loss, 2003). The basic prediction of a resistance sensitive to the relative polarizations has recently been verified experimentally, as has the exponential decay of the effect on the scale of the coherence length (Beckmann *et al.*, 2004). The amplitude of the effect is sensitive to the exact geometry and to scattering inside the superconductor (Melin and Feinberg, 2002).

VII. CONCLUSIONS

ASJ reflections are a powerful tool for the study of the nature of electronic excitations in superconductors, determination of energy-gap values, and studies of the symmetry of the order parameter. Strong ASJ reflections have been observed in all cuprates tested so far, including in the underdoped pseudogap regime. Because their occurrence implies electron-hole mixing, it follows that the nature of electronic excitations in the cuprates is similar to that in ordinary metals. This is an important result, which can help to discriminate between the predictions of different theoretical high-T_c superconductor models. From the energy dependence of ASJ reflections, one can infer that the scale of coherent, homogeneous superconductivity is on the order of 20 meV. Pseudogap values substantially exceeding this value may not be related directly to superconductivity, and are apparently characteristic of the antinode directions. If the pseudogap is a high-temperature precursor of superconductivity, it must be strongly momentum dependent. The same holds if it is the manifestation of a competing order. ASJ doping dependence gives indications for the existence of an additional interaction channel, besides the one giving rise to *d*-wave symmetry. This additional channel becomes stronger as doping is increased beyond optimum doping. ASJ spectroscopy under applied magnetic fields provides a tool for the study of surface currents, including Meissner currents due to an effective Bean-Livingston barrier against vortex penetration, and currents possibly linked to an imaginary component of the order parameter induced by the magnetic field.

ACKNOWLEDGMENTS

I am greatly indebted to Philippe Nozières and to Fabio Pistolesi for numerous illuminating discussions and for giving me access to their unpublished results on Andreev–Saint-James reflections in the strong-coupling regime. Many thanks are due to Jacques Friedel for his patient explanations on the origin of the pseudogap concept and to Roger Maynard for many fruitful discussions on ASJ reflections and related topics. Much help from and discussions with Meir Weger, Bernard Raveau, and Alex Revcolevschi are gratefully acknowledged. A special thank is due to Amir Kohen and to Roy Beck for providing a number of useful numerical simulations, and to Roy Beck for his invaluable technical help with preparation of the figures. The major part of this review was prepared while I was a guest at the Institut Laue-Langevin, which I would like to thank for its support. I would also like to thank warmly Efim Kats for his hospitality during this stay, and for many interesting discussions. Finally, I would like to thank Yoram Dagan, Amir Kohen, Roy Beck, and Guy Leibovitch of the Tel Aviv team, and Oded Millo and Gad Koren for their many contributions to this work. Support from the Israel Science Foundation, from the Heinrich Hertz-Minerva Center for High-Temperature Superconductivity, and from the Oren Family Chair for Experimental Solid-State Physics is gratefully acknowledged.

REFERENCES

Achsaf, N., G. Deutscher, A. Revcolevschi, and M. Okuya, 1996, in *Coherence in High Temperature Superconductors*, edited by G. Deutscher and A. Revcolevschi (World Scientific, Singapore), p. 428.

Alexandrov, A. S., and A. F. Andreev, 2001, Europhys. Lett. **54**, 373.

Alexandrov, A. S., and N. F. Mott, 1994, Rep. Prog. Phys. **57**,

1197.
Alff, L., Y. Krockenberger, B. Welter, M. Schonecke, R. Gross, D. Manske, and M. Naito, 2003, Nature (London) **422**, 698.
Alff, L., H. Takashima, S. Kashiwaya, N. Terada, T. Ito, K. Oka, Y. Tanaka, and M. Koyanagi, 1997, Physica C **282-287**, 1485.
Alloul, H., T. Ohno, and P. Mendels, 1989, Phys. Rev. Lett. **63**, 1700.
Altman, E., and A. Auerbach, 2002, Phys. Rev. B **65**, 104508.
Anderson, P., 1987, Science **235**, 1196.
Andreev, A., 1964, Zh. Eksp. Teor. Fiz. **46**, 1823 [Sov. Phys. JETP **19**, 1228].
Aprili, M., E. Badica, and L. Greene, 1999, Phys. Rev. Lett. **83**, 4630.
Aubin, H., L. H. Greene, S. Jian, and D. G. Hinks, 2002, Phys. Rev. Lett. **89**, 177001.
Bean, C., and J. Livingston, 1968, Phys. Rev. Lett. **12**, 14.
Beck, R., 2004, private communication.
Beck, R., Y. Dagan, A. Milner, A. Gerber, and G. Deutscher, 2004, Phys. Rev. B **69**, 144506.
Beck, R., A. Kohen, G. Leibovitch, H. Castro, and G. Deutscher, 2003, J. Low Temp. Phys. **131**, 451.
Beckmann, D., H. Weber, and H. Lohneysen, 2004, Phys. Rev. Lett. **93**, 197003.
Benfatto, L., S. Caprata, and C. Castro, 2000, Eur. Phys. J. B **17**, 95.
Bernevig, B., G. Chapline, R. Laughlin, Z. Nazario, and D. Santiago, 2003, cond-mat/0312573.
Bernhard, C., *et al.*, 1995, Phys. Rev. B **52**, 10488.
Blonder, G. E. and M. Tinkham, 1983, Phys. Rev. B **27**, 112.
Blonder, G. E., M. Tinkham and T. M. Klapwijk, 1982, Phys. Rev. B **25**, 4515
Bogoliubov, N., 1947, J. Phys. (Moscow), **11**, 23.
Bogoliubov, N., 1958, Zh. Eksp. Teor. Fiz. **34**, 58 [Sov. Phys. JETP **7**, 41 (1958)].
Buchholz, L., and G. Zwicknagl, 1981, Phys. Rev. B **23**, 5788.
Bussieres, J., 1976, Phys. Lett. **58A**, 343.
Caroli, C., P. de Gennes, and J. Matricon, 1964, Phys. Lett. **9**, 307.
Castellani, C., C. di Castro, and M. Grilli, 1997, Z. Phys. B: Condens. Matter **103**, 137.
Chen, Q., J. Stajic, A. Tan, and K. Levin, 2004, cond-mat/0404274.
Chen, Z., A. Biswas, I. Uti, T. Wu, S. B. Ogale, R. L. Greene, and T. Venkatesan, 2001, Phys. Rev. B **63**, 212508.
Covington, M., M. Aprili, E. Paraonu, L. Greene, F. Xu, J. Zhu, and C. Mirkin, 1997, Phys. Rev. Lett. **79**, 277.
Dagan, Y., and G. Deutscher, 2001a, Phys. Rev. Lett. **87**, 177004.
Dagan, Y., and G. Deutscher, 2001b, Phys. Rev. B **64**, 092509.
Dagan, Y., A. Kohen, G. Deutscher, and A. Revcolevschi, 2000, Phys. Rev. B **61**, 7012.
Daghero, D., R. Gonelli, G. Ummarino, and V. Stepanov, 2002, cond-mat/0207411.
de Gennes, P., 1966, *Superconductivity of Metals and Alloys* (Benjamin, New York), p. 137.
de Gennes, P., and D. Saint-James, 1963, Phys. Lett. **4**, 151.
de Jong, M. J. M., and C. W. J. Beenakker, 1995, Phys. Rev. Lett. **74**, 1657.
Deutscher, G., 1999, Nature (London) **397**, 410.
Deutscher, G., and P. de Gennes, 1969, in *Superconductivity*, edited by R. Parks (Dekker, New York), p. 1005.
Deutscher, G., and D. Feinberg, 2000, Appl. Phys. Lett. **76**, 487.
Deutscher, G., and R. Maynard, 1998, in *The Gap Symmetry and Fluctuations in High-T_c Superconductors: Proceedings of a NATO Advanced Study Institute Summer School*, Cargese, Corsica, 1997, edited by J. Bok, G. Deutscher, D. Pavuna, and S. Wolf, NATO Advanced Study Institute, Series, B: Physics. No. 371 (Plenum, New York), p. 537.
Deutscher, G., and P. Nozières, 1994, Phys. Rev. B **50**, 13 557.
D'Gorno, I., and A. Kohen, 1998, unpublished.
Ding, H., M. Norman, T. Machiku, K. Kadowaki, and J. Giapinzakis, 1996, Nature (London) **382**, 51.
Dong, Z., R. Ramesh, and T. Venkatesan, 1997, Appl. Phys. Lett. **71**, 1718.
Emery, V., and S. Kivelson, 1995, Nature (London) **374**, 434.
Ernst, G., A. Nowack, M. Weger, and D. Schweizer, 1994, Europhys. Lett. **25**, 303.
Fischer, O., C. Renner, and I. M. Aprile, 1998, in *The Gap Symmetry and Fluctuations in High-T_c Superconductors: Proceedings of a NATO Advanced Study Institute Summer School*, Cargese, Corsica, 1997, edited by J. Bok, G. Deutscher, D. Pavuna, and S. Wolf, NATO ASI Series, B, No. 371 (Plenum, New York), p. 487.
Fogelstrom, M., D. Rainer, and J. Sauls, 1997, Phys. Rev. Lett. **79**, 281.
Fogelstrom, M., D. Rainer, and J. Sauls, 2004, Phys. Rev. B **70**, 012503.
Fournier, P., E. Maiser, and R. Greene, 1998, in *The Gap Symmetry and Fluctuations in High-T_c Superconductors: Proceedings of a NATO Advanced Study Institute Summer School*, Cargese, Corsica, 1997, edited by J. Bok, G. Deutscher, D. Pavuna, and S. Wolf, NATO Advanced-Study Institute, Series B: Physics, No. 371 (Plenum, New York), p. 145.
Friedel, J., 2004, private communication.
Friedberg, R., and T. Lee, 1989, Phys. Rev. B **40**, 6745.
Friedel, J., 1988, Physica C **153**, 1610.
Friedel, J., 1989, J. Phys.: Condens. Matter **1**, 7757.
Friedel, J., and M. Kohmoto, 2002, Eur. Phys. J. B **30**, 427.
Fu, C., Z. Huang, and N.-C. Yeh, 2002, Phys. Rev. B **65**, 224516.
Giaever, I., 1960, Phys. Rev. Lett. **5**, 147.
Goll, G., H. Lohneysen, I. Yanson, and L. Taillefer, 1993, Phys. Rev. Lett. **70**, 2008.
Griffin, A., and J. Demers, 1971, Phys. Rev. B **4**, 2202.
Hass, N., G. Deutscher, A. Revcolevschi, and G. Dhalenne, 1994, J. Supercond. **7**, 763.
Hass, N., D. Ilzycer, G. Deutscher, G. Desgardin, I. Monot, and M. Weger, 1992, J. Supercond. **5**, 191.
Hass, N., D. Ilzycer, G. Deutscher, G. Desgardin, I. Monot, and M. Weger, 1993, Physica C **209**, 85.
Hasselbach, K., J. Kirtley, and J. Lejay, 1993, Physica B **186-188**, 201.
Hu, C.-R., 1994, Phys. Rev. Lett. **72**, 1526.
Junod, A., A. Erb, and C. Renner, 1999, Physica C **317-318**, 333.
Kashiwaya, S., and Y. Tanaka, 2000, Rep. Prog. Phys. **63**, 1641.
Kashiwaya, S., Y. Tanaka, M. Koyanagi, H. Takashima, and K. Kajimura, 1995, Phys. Rev. B **51**, 1350.
Kashiwaya, S., Y. Tanaka, N. Yoshida, and M. Beasley, 1999, Phys. Rev. B **60**, 3572.
Kleefisch, S., B. Welter, A. Marx, L. Alff, R. Gross, and M. Naito, 2001, Phys. Rev. B **63**, 100507(R).
Kohen, A., G. Leibovitch, and G. Deutscher, 2003, Phys. Rev. Lett. **90**, 207005.

Krupke, R., and G. Deutscher, 1999, Phys. Rev. Lett. **83**, 4634.
Laughlin, R., 1998, Phys. Rev. Lett. **80**, 5188.
Laughlin, R., 2002, cond-mat/0209269.
Leggett, A., 1980, in *Modern Trends in the Theory of Condensed Matter*, edited by A. Bekalsky and J. Przyspawa (Springer, Berlin), p. 13.
Lesueur, J., L. Greene, W. Feldmann, and I. Inam, 1992, Physica C **191**, 325.
Marcenat, C., R. Calemszuk, and A. Carrington, 1996, in *Coherence in High Temperature Superconductors*, edited by G. Deutscher and A. Revcolevschi (World Scientific, Singapore), p. 101.
Margaritondo, J., 1998, in *The Gap Symmetry and Fluctuations in High-T_c Superconductors: Proceedings of a NATO Advanced Study Institute Summer School*, Cargese, Corsica, 1997, edited by J. Bok, G. Deutscher, D. Pavuna, and S. Wolf, NATO Advanced-Study Institute, Series B: Physics (Plenum, New York), p. 195.
Marmi, M., F. Pistolesi, and G. Strinati, 1998, Eur. Phys. J. B **1**, 151.
Massida, S., J. Yu, K. Park, and A. Freeman, 1991, Physica C **176**, 159.
McElroy, K., D.-H. Lee, J. E. Hoffman, K. M. Lang, E. W. Hudson, H. Eisaki, S. Uchida, J. Lee, and J. Davis, 2004, cond-mat/0404005.
McMillan, W., and J. M. Rowell, 1969, in *Superconductivity*, edited by R. D. Parks (Dekker, New York), p. 561.
Melin, R., and D. Feinberg, 2002, Eur. Phys. J. B **26**, 101.
Mendelssohn, K., and J. Olsen, 1950, Phys. Rev. **80**, 859.
Merril, R., and Q. Si, 1999, Phys. Rev. Lett. **83**, 5326.
Miyakawa, N., P. Guptasarma, and J. Zasadzinski, 1997, Phys. Rev. Lett. **80**, 157.
Muller, K. A., 2004, J. Supercond. **17**, 3.
Ng, T. K., and C. M. Varma, 2004, Phys. Rev. B **70**, 054517.
Ngai, J., 2004, Appl. Phys. Lett. **84**, 1908.
Nozières, P., and F. Pistolesi, 1999, Eur. Phys. J. B **10**, 649.
Nozières, P., and S. Schmitt-Rink, 1985, J. Low Temp. Phys. **59**, 195.
Okashi, I., and A. Kohen, 2002, private communication.
Pankove, J., 1966, Phys. Lett. **21**, 406.
Perali, A., C. Castellani, C. di Castro, M. Grilli, E. Piegari, and A. A. Varlamov, 2000, Phys. Rev. B **62**, R9295.
Pistolesi, F., 1998, unpublished.
Pistolesi, F., and P. Nozières, 2000, unpublished.
Pistolesi, F., and G. Strinati, 1996, Phys. Rev. B **53**, 15 168.
Pryadko, L., S. Kivelson, and O. Zachar, 2004, Phys. Rev. Lett. **92**, 067002.
Qazilbash, M., A. Biswas, Y. Dagan, R. Ott, and R. Greene, 2003, Phys. Rev. B **68**, 024502.
Racah, D., and G. Deutscher, 1996, Physica C **263**, 218.
Ranninger, J., J. Robin, and M. Eschrig, 1995, Phys. Rev. Lett. **74**, 4027.
Recher, P., and D. Loss, 2003, Phys. Rev. Lett. **91**, 267003.
Renner, C., B. Revaz, J.-Y. Genoud, K. Kadowaki, and Ø. Fisher, 1997, Phys. Rev. Lett. **80**, 149.
Sachdev, S., 2000, Science **288**, 475.
Saint-James, D., 1964, J. Phys. (Paris) **25**, 899.
Sharoni, A., G. Koren, and O. Millo, 2001, Europhys. Lett. **54**, 675.
Sharoni, A., G. Leibovitch, A. Kohen, R. Beck, G. Deutscher, G. Koren, and O. Millo, 2003, Europhys. Lett. **62**, 883.
Sharoni, A., O. Millo, A. Kohen, Y. Dagan, R. Beck, G. Deutscher, and G. Koren, 2002, Phys. Rev. B **65**, 134526.
Sharvin, Y., 1965, Zh. Eksp. Teor. Fiz. **48**, 984 [Sov. Phys. JETP **21**, 655 (1965)].
Sinha, S., and K.-W. Ng, 1998, Phys. Rev. Lett. **80**, 1296.
Skinta, J., M. Kim, T. Lemberger, T. Greibe, and M. Naito, 2002, Phys. Rev. Lett. **88**, 207005.
Soulen, R., *et al.*, 1998, Science **282**, 85.
Tallon, J., and J. Loram, 2001, Physica C **349**, 53.
Tanaka, Y., 1996, in *Coherence in High Temperature Superconductors*, edited by G. Deutscher and A. Revcolevschi (World Scientific, Singapore), p. 393.
Tanaka, Y., and S. Kashiwaya, 1995, Phys. Rev. Lett. **74**, 3451.
Timusk, T., and B. Statt, 1999, Rep. Prog. Phys. **62**, 61.
Tsuei, C. C., and J. R. Kirtley, 2000a, Rev. Mod. Phys. **72**, 969.
Tsuei, C. C., and J. R. Kirtley, 2000b, Phys. Rev. Lett. **85**, 182.
Uemura, Y. J., 2003, Solid State Commun. **126**, 23.
Upadhyay, S. K., A. Palanisami, R. N. Louie, and R. A. Buhrman, 1998, Phys. Rev. Lett. **81**, 3247.
Vas'ko, V. A., V. A. Larkin, P. A. Kraus, K. R. Nikolaev, D. E. Grupp, C. A. Nordman, and A. M. Goldman, 1997, Phys. Rev. Lett. **78**, 1134.
Walker, M., and P. Pairor, 1999, Phys. Rev. B **59**, 1421.
Wei, J., N.-C. Yeh, D. Garrigas, and M. Strasik, 1998, Phys. Rev. Lett. **81**, 2542.
Wolf, S., 1971, Ph.D. thesis (Rutgers University).
Wollman, D., D. van Harlingen, W. Lee, D. Ginsberg, and A. Leggett, 1993, Phys. Rev. Lett. **71**, 2134.
Yagil, Y., N. Hass, G. Desgardin, and I. Monot, 1995, Physica C **250**, 59.
Yang, J., and C.-R. Hu, 1994, Phys. Rev. B **50**, 16 766.
Zaitsev, A., 1980, Sov. Phys. JETP **51**, 111.
Zavaritskii, N., 1960, Zh. Eksp. Teor. Fiz. **38**, 1673 [Sov. Phys. JETP **38**, 1673].
Zhu, J., B. Friedman, and C. Ting, 1999, Phys. Rev. B **59**, 9558.
Zutic, I., J. Fabian, and S. das Sarma, 2004, Rev. Mod. Phys. **76**, 323.
Zutic, I., and O. T. Valls, 1999, Phys. Rev. B **60**, 6320.
Zutic, I., and O. T. Valls, 2000, Phys. Rev. B **61**, 1555.